1984

Final report on I79 tied arch cracking - neville island bridge, December 1984 82p

John W. Fisher

Alan W. Pense

Craig C. Menzemer

Eric J. Kaufmann

Lehigh University

FINAL REPORT ON I79 TIED ARCH CRACKING - NEVILLE ISLAND BRIDGE

by
John W. Fisher
Alan W. Pense
Craig C. Menzemer
Eric J. Kaufmann

Fritz Engineering Laboratory

Report No. 494-1(84)

72-101

REPORT DOCUMENTATION PAGE	1. REPORT NO. FHWA/PA-84-016	2.	3. Recipient's Accession No.

Title and Subtitle

FINAL REPORT ON I79 TIED ARCH CRACKING
- NEVILLE ISLAND BRIDGE

5. Report Date: December 1984

6.

Author(s) John W. Fisher, Alan W. Pense,
Craig C. Menzemer, Eric J. Kauffman

8. Performing Organization Rept. No. 494-1(84)

Performing Organization Name and Address

Fritz Engineering Laboratory, #13
Lehigh University
Bethlehem, Pennsylvania 18015

10. Project/Task/Work Unit No. 83-27

11. Contract(C) or Grant(G) No.
(C) 77500
(G)

Sponsoring Organization Name and Address

Department of Transportation
Harrisburg, Pennsylvania 17120

13. Type of Report & Period Covered
Final Report
Feb. 1984 to Feb. 1985

14.

Supplementary Notes

Abstract (Limit: 200 words)

Cracks were detected in the diaphragm to tie girder web welds of the I79 Neville Island Bridge in July 1983. These cracks were observed at the top and bottom ends of the transverse welds between the diaphragm and the outside plate at floor beams. Samples removed from these cracked regions showed that all of these cracks developed from lack of fusion in the welded connections. Cyclic stresses developed in the diaphragms normal to these welds resulted in fatigue crack growth.

Strain measurement under random truck traffic demonstrated that the web gap at all four box corners were subjected to large distortion induced stresses. Removal of the loading bar at a typical joint verified that crack growth had occurred. Connecting the diaphragm to the top and bottom tie girder flanges prevented distortion in the outside tie girder web. However, it did not reduce the distortion induced cyclic stresses at the bottom inside connection. It was found necessary to provide a positive bolted splice between the floor beam flange and the tie girder flange.

Document Analysis a. Descriptors

Bridges, Connections, Design, Distortion, Fabrication, Fatigue cracks, Retrofit, Weld defects

b. Identifiers/Open-Ended Terms

c. COSATI Field/Group

Availability Statement	19. Security Class (This Report)	21. No. of Pages
		82
	20. Security Class (This Page)	22. Price

COMMONWEALTH OF PENNSYLVANIA

Department of Transportation

Office of Research and Special Studies

Project 83-27

FINAL REPORT ON I79 TIED ARCH CRACKING

- NEVILLE ISLAND BRIDGE

by

John W. Fisher

Alan W. Pense

Craig C. Menzemer

Eric J. Kaufmann

Prepared in cooperation with the Pennsylvania Department of Transportation and the U. S. Department of Transportation, Federal Highway Administration. The contents of this report reflect the views of the authors who are responsible for the facts and the accuracy of the data presented herein. The contents do not necessarily reflect the official views or policies of the Pennsylvania Department of Transportation or the U. S. Department of Transportation, Federal Highway Administration. This report does not consitute a standard, specification, or regulation.

Lehigh University

Office of Research

Bethlehem, Pennsylvania

December 1984

Fritz Engineering Laboratory Report No. 494-1(84)

ACKNOWLEDGMENTS

This investigation was part of Fritz Engineering Laboratory Project 494 sponsored by the Pennsylvania Department of Transportation and the Federal Highway Administration.

The study was conducted at the Fritz Engineering Laboratory and Whitaker Laboratory, Lehigh University, Bethlehem, Pennsylvania. The authors wish to acknowledge the help provided by Messrs. Harry Laatz and Ronald Nelson of the Federal Highway Administration who obtained the initial strain measurements in September 1983. Thanks are also due Dr. B. T. Yen and Mr. Hugh T. Sutherland for their assistance with the strain measurements that were acquired in April 1984.

Appreciation is also due Mrs. Ruth Grimes for typing the manuscript, Mr. Jack Gera for preparation of the line drawings and Mr. Richard Sopko for his photographic work.

1. INTRODUCTION

Cracks detected in the tie girders of the I470 bridge in Wheeling, West Virginia were found to occur at the diaphragm where floor beams framed into the tie girders. Since the I79 tie girder structure at Neville Island was similar in details, an examination was made of similar connections, and inspection was made of that structure as well. Figure 1a shows a map of the area around the Neville Island bridge crossing. The 750 ft. tied arch structure spans the main channel between Neville Island and the east side of the river. Figure 1b shows the bridge elevation. Similar cracks (nine total) were found to exist in the welded connection between the diaphragm and outside web of the tie girders in July 1983[1].

As a result of the cracking that was detected in the diaphragm - tie girder web welded connections, the Pennsylvania Department of Transportation requested the Federal Highway Administration to obtain field measurements and J. W. Fisher and his staff at Lehigh University to prepare a proposal to evaluate the test results, assess the causes of the cracking, evaluate retrofit procedures and provide recommendations as appropriate.

In order to aid in assessing the cause of the diaphgram - web welded connection, strain gages were installed in the upstream tie girder at panel points 13 and 14 and strain measurements were acquired under random truck traffic during the period September 14 to 17, 1983.*

---

*The field instrumentation and measurements were carried out by Messrs. Harry Laatz and K. Nelson of the Turner Fairbanks Highway Research Center of the Federal Highway Administration.

A retrofit procedure was proposed by Richardson, Gordon and Associates after discovery of the cracked welds which consisted of drilling holes in the diaphragm at the crack tips where cracks were discovered and installing two 7 x 4 x 1/2 x in. x 2 ft. - 9 in. angles between the top and bottom flange plates[2]. At panel points with bolted flange splices 5 x 5 x 1/2 in. x 2 ft. - 3 in. angles were used. The angles were bolted into place after the paint was removed and holes drilled so that friction-type joints resulted. The tie girders were inspected at each floor beam diaphragm[3], and these retrofit angles were installed in February - April 1984.

During the inspection and initial retrofit several samples were removed from the diaphragm which included all or part of the cracked welded connection. These segments were evaluated and examined to determine the causes of crack growth.

After the April 1984 retrofit was completed, additional measurements were obtained on the retrofitted connections in order to establish the adequacy of the retrofit. These measurements were obtained by Lehigh personnel during the week of April 16, 1984.

This report summarizes the results of all of the field measurements and assesses the significance of the cracking. Recommendations are also provided.

2. STRAIN MEASUREMENTS UNDER RANDOM TRUCK TRAFFIC PRIOR TO RETROFIT

2.1 Instrumentation

In order to aid in assessing the cracking that developed in the floor beam diaphragm weld to web connections, strain gages were installed at panel points 13 and 14 of the upstream tie girder. Sixteen gages were installed in the web gaps and on the diaphragm at panel point 13, as illustrated in Fig. 2. Three gages were insalled in the top and bottom web gaps of the outside web and five in the inside web gap (two at the top and three at the bottom). Four of the remaining gages were installed on the diaphragm and one on the center of the bottom flange.

At panel point 14, the same general location of gages was maintained, as shown in Fig. 3. The only difference was the distribution of gages in the web gaps of the outside web. As shown in Fig. 3, four gages were placed in the bottom web gap and two in the top web gap.

2.2 Test Results and Analysis

Measurements were acquired from random trucks crossing the structure in the north and southbound lanes. Table 1 summarizes the 29 sets of measurements and shows the type of truck and its lane position as it crossed the structure. Figures 4 and 5 show examples of the strain-time response observed in the web gaps, diaphragm and bottom flange. Gages in the web gaps and on the diaphragms show large stress cycles that include significant stress reversal. It is evident that one or more trucks crossing the floor beam produce a major stress cycle in these components.

As the largest cracks were observed at the upper outside corner, historgrams of gages C1 and C5 at PP 13 and 14 (see Figs. 2 and 3) which were mounted on the diaphragms were constructed. These results are summarized in Figs. 6 and 7. These measurements indicated that the effective stress range acting on the transverse weld was about 2.8 ksi.

The histograms for the gages with the higher responses in the web gaps at panel points 13 and 14 are summarized in Figs. 8 and 9. The maximum stress range observed at these gages was between 8 and 11 ksi at panel point 14 and between 2.5 and 9 at panel point 13.

The strain measurements indicated that significant stress gradients existed in the web gaps at all four corners. Gradients in the web gaps at the maximum and minimum response during the larger stress cycles were constructed (Figs. 10 to 16). The difference between the maximum and minimum response is equal to the stress range for that stress excursion. The results indicate that most of the web gaps are distorted into double curvature. This indicates the web is being displaced out-of-plane relative to the top and bottom flanges, as illustrated schematically in Figs. 17 and 18 for the maximum and minimum response positions (see Figs. 4 and 5).

The distorted shapes corresponding to the strain measurements suggest that the floor beam introduces a reversal of end moment into the tie girder diaphragm connection.

The extrapolation of the stress gradients to the root area of the web - flange weld under the backing bar demonstrates that high stress range occurrences are occurring at those locations and at the termination of the

welds attaching the diaphragm to the outside web. Table 2 provides a summary of the peak stress ranges observed in the diaphragm and in the web gaps.

The extrapolated web gap stresses indicate that the stress range that is developed at the backing bar weld root is significantly greater than the stress range spectrums shown in Figs. 8 and 9. At panel point 13, the extrapolated stress range is four times as great in the upper outside corner and about 1.5 times as great elsewhere. At panel point 14, these values were observed to be nearly three times as large.

These levels of stress range are large enough to result in crack propagation into the girder webs, particularly at the weld root areas shown schematically in Fig. 18.

The stress range observed in the bottom flange of the upstream tie girder at panel points 13 and 14 is summarized in Figs. 19 and 20. The measurements indicate that the stress range at panel point 13 is slightly higher than at panel point 14. The maximum stress range at panel point 13 was 2.3 ksi and 1.4 ksi at panel point 14. It is also apparent from Fig. 5 that few stress range excursions occur in the tie girder then in the web gaps and diaphragms.

3. STRAIN MEASUREMENTS UNDER RANDOM TRAFFIC AFTER INITIAL RETROFIT

The initial retrofit consisted of pairs of 7 x 4 x 1/2 in. angles connected to the diaphragm and top and bottom flanges, as illustrated in Fig. 21. At several locations the cracked weld had been removed, as illustrated in Fig. 22.

3.1 Instrumentation

In order to evaluate the effectiveness of the initial retrofit, strain gages were installed on the tie girder web gaps at panel points 13 and 14 during the week of April 16, 1984. Figures 23 and 24 show schematics of the gage locations at the two panel points. In addition to the gages installed inside the box, several gages were installed on the outside of the bottom outside web plate in the gap region. This permitted the gradient to be examined through the web thickness. It was not possible to install gages at the other outside corner because of the existence of the hanger plates and the floor beam.

Figures 25 and 26 show the strain gages installed inside the tie girder at the web gaps of the bottom inside and outside webs. The backing bar at each corner is easily seen in each print.

3.2 Test Results and Analysis

Strain measurements were acquired for about 12 hours of random truck traffic. Figure 27 shows typical stress - time responses observed in the web gaps with the retrofit angles in place. The results show that

negligible stresses are developed in the outside web gap. In general the observed stresses were less than 1 ksi. Table 3 summarizes the maximum stress ranges observed in the gages at panel points 13 and 14. It is apparent that only the inside bottom web gap has not been affected significantly by the installation of the retrofit angles.

Figure 28 compares the gradient in the bottom outside web gap at panel point 14 before and after the retrofit. A significant reduction in the gap distortion is apparent. The retrofit reduced the stress range in the outside web gaps by 80 - 90%. The cyclic stresses were reduced to a tolerable level which will prevent additional cracks from forming in the diaphragm-web connections and the tie girder webs. Figures 29 and 30 show the strain gradients observed in the inside bottom web gap at panel point 14. A comparison of Figs. 29 and 30 with Fig. 16 demonstrates that the retrofit had little effect on the web gap distortion. There was no significant difference observed in the web gap stresses at the floor beam connections.

Figure 31 shows the stress range histogram for the bottom web gap gage at panel point 14. A comparison of this histogram after the retrofit with the results shown in Fig. 9 also demonstrates that the bottom web gap was not affected by the retrofit. Hence, continued crack growth could be expected at the backing bar weld root.

The strain measurements verified that additional steps must be taken to prevent web gap distortion. The observed stresses in the bottom web gap were observed to exceed the fatigue resistance of the weld root at the web-flange weld. The desired reduction in this web gap can be accomplished

by providing a connection between the floor beam bottom flange and the tie girder bottom flange. A bolted strap will prevent distortion in this web gap and can be expected to reduce the cyclic stress to a level comparable to the outside web gaps.

4. EXAMINATION OF THE FLOOR BEAM DIAPHRAGM - TIE GIRDER WEB WELD CRACKS

Nine samples were removed from the tied arch box tie girder diaphragms for examination and fractographic analysis. All of these samples came from the welded connection to the outside web. They were removed from panel points T1A-NB top and bottom, T2A-NB top and bottom, T4-NB bottom, and T1-NB top of the upstream tie, and from panel points T4A-SB bottom, T2-SB bottom, and T1-SB bottom of the downstream tie girder.

One of the cracks was found to have turned into the girder web. This occurred at panel point T1-NB top of the upstream tie. The crack was observed to turn into the girder web about 1-1/2 in. below the end of the diaphragm. A 3 in. diameter hole saw was used to remove this crack. The core included the outside hanger splice plate.

Each of the samples was examined and photographed, and the lack of fusion and fatigue cracked regions defined.

Several of the crack surfaces were examined in detail with the scanning and/or the transmission electron microscope. Samples removed from T1A-NB top and T2A-NB top were selected for these studies.

In addition several of the plate cross-sections were polished and etched in order to define the crack path and lack of fusion conditions.

4.1 General Appearance of the Samples

Most of the samples were removed by cutting a hole in the diaphragm and then saw cutting into the cracked region. Figures 32 to 52 show the

segments and their crack surfaces. It is readily apparent from most of the crack surfaces that large unfused areas existed in the groove weld that connected the diaphragm to the tie girder web at the top and bottom web gaps. The original flame cut edge is visible on many of these surfaces (see Figs. 33, 35, 37, 39, 42, 48, 50 and 52). Furthermore, many of the weld joints do not appear to be beveled. As a result, very shallow surface welds appeared to exist along the edges of the diaphragm and web, much like small fillet welds.

The observed lack of fusion at the ends of the diaphragm-web welds are not in accord with the weld joint called for on the design and fabrication drawings. However, considering the accessibility of these locations and the fact that the welds were not ultrasonically tested during production, the observed deviations would appear to be inevitable. The failure to bevel the diaphragm as observed at several locations is not an acceptable procedure.

4.2 Metallographic Studies and Cross-Sections

Several of the segments were cut perpendicular to the lack of fusion area, so that the cross-section could be polished and etched. This permitted the groove preparation, lack of fusion and weldments to be examined. The location of the polished section is shown by the dashed lines in Figs. 33, 35, 40, 42, 44 and 50.

Photomicrographs of T1A-NB bottom, T2A-NB top and T4-NB bottom (see Figs. 55, 56 and 57) do not show any evidence of beveled edges. Figures

show that a single bevel groove was prepared. None of the sections at the end of the diaphragm show significant amounts of fusion. The lack-of-fusion depth varied from 0.3 to 0.5 in. In nearly all cases this resulted in fatigue crack growth from the unfused weld root, as the crack extended through the weld ligaments to the free surface.

In many cases the lack of fusion decreased away from the end of the diaphragm. This is apparent in Figs. 35, 44, 50 and 52. In the case of the samples shown in Figs. 37 and 39, the lack of fusion extended over much longer lengths.

It is apparent that the lack of fusion was primarily responsible for the fatigue crack propagating from the weld root. The weld toe crack shown in Fig. 53 can be seen to extend over several inches in Fig. 35. Root cracking can also be observed on the other side of the diaphragm plate.

The fatigue crack turned and propagated into the web plate at panel point T1-NB top (see Fig. 46). The core sample was milled to the crack tip, as shown in Fig. 60. This showed that the crack had propagated about halfway through the web thickness. A view of the crack tip at high magnification can be seen in Fig. 61.

4.3 Fractographic Studies

The fracture surface area of several samples were examined for evidence of the nature of the fracture process involved. The results of these studies are seen in Figs. 63 to 68. Scanning electron micrographs of portions from samples T1A-NB and T2A-NB showed evidence of fatigue

crack growth. The evidence of fatigue crack growth is clear from the beach marks seen in Figs. 63 and 66. Striations can be clearly seen in Figs. 64 and 67.

Transmission electron micrographs were also prepared from replicas taken from the crack surfaces. These fatigue striations are clearly seen in Fig. 65 and 68. The fatigue crack growth developed at high ΔK levels. From the striation spacing in Figs. 65 and 68, it appears that the crack growth rates are between 2 and 5 x 10^{-6} in/cycle for the cracks observed in T1A-NB top and T2A-NB top.

5. ANALYSIS OF CRACK PROPAGATION

Near the ends of the diaphragm - outer web transverse welds, significant evidence of lack of fusion was observed between the roots of the weld passes along each surface of the diaphragm. The unfused thickness of the 1/2 in. diaphragm plate and the small "seal" welds provide a large crack-like defect that is parallel to the primary stresses in the tie girder and hence has no affect on the tie girder. However, as the strain measurements from normal traffic have demonstrated, a cyclic stress range is developed in the diaphragm, and this cyclic stress is perpendicular to the lack of fusion area.

The stress intensity factor for this lack of fusion condition can be estimated from the equation[4].

$$\frac{K\left(A_1 + A_2 \frac{a}{w}\right) \sigma \sqrt{\pi a \sec \frac{\pi a}{2w}}}{1 + \frac{2H}{t_p}} \qquad (1)$$

where $W = H + \frac{t_p}{2}$

$$A_1 = 0.528 + 3.287\left(\frac{H}{t_p}\right) - 4.361\left(\frac{H}{t_p}\right)^2 + 3.696\left(\frac{H}{t_p}\right)^3 - 1.875\left(\frac{H}{t_p}\right)^4 + 0.415\left(\frac{H}{t_p}\right)^5$$

$$A_2 = 0.218 + 2.717\left(\frac{H}{t_p}\right) - 10.171\left(\frac{H}{t_p}\right)^2 + 13.122\left(\frac{H}{t_p}\right)^3 - 7.755\left(\frac{H}{t_p}\right)^4 + 1.783\left(\frac{H}{t_p}\right)^5$$

At the diaphragm ends, the value of H was observed to be between 0.06 and 0.15 in. The unfused widths corresponding to the initial crack size, 2a, varied between 0.4 in. and 0.5 in.

The crack and geometric conditions indicate that stress cycles between 1.5 and 2.5 ksi will result in fatigue crack growth if Eq. 1 is equated to the crack growth threshold taken as $\Delta K = 2.75$ ksi $\sqrt{\text{in.}}$ for the various lack of fusion and weld sizes observed.

The striation spacing observed during the fractographic examination indicated that the growth rate varied from 2 to 5 x 10^{-6} in/cycle. This rate of growth was detected near the lower end of the diaphragm.

If the crack growth is equated to the relationship

$$\frac{da}{dN} = 3.6 \times 10^{-10} \Delta K^3 \qquad (2)$$

stress intensity ranges between 15 ksi $\sqrt{\text{in.}}$ and 24 ksi $\sqrt{\text{in.}}$ result. This corresponds to a stress range of 5 to 15 ksi depending on the crack size.

The results of the fracture surface examination suggests that the stress range that resulted in crack growth was higher than the stress cycles produced by random trucks. This is not unusal since only the higher stress cycles result in detectable striations.

6. OBSERVATIONS IN THE WEB GAP

In order to assess the effects of the web gap bending distortion, segments of the backup bars were removed from the bottom outside box corners at the diaphragm.

The web - flange weld fused into a backing bar, as shown schematically in Fig. 69. Web gap bending stresses can result in fatigue crack growth from the weld root (see Fig. 69), and from the lack of fusion between the backing bar and flange.

Figure 70 shows a photograph of the web gap and part of the weld remaining after the backing bar was removed.

The "weld toe" along the web that remained after removal of the backing bar and the toe at the lack of fusion plane on the flange surface were ground, as illustrated in Fig. 71. This removed the weld toe from the girder web and also removed more than 1/8 in. of the weld at the flange surface. The ground areas were then treated with liquid penetrant, as illustrated in Fig. 72. This demonstrated that fatigue crack growth had developed in the girder web and that the lack of fusion plane on the flange surface had been extended, as can be seen in Figs. 72 and 73.

None of these crack extensions are significant since they lie in a plane parallel to the primary stresses in the tie girder and the structure has been retrofitted to prevent further web-gap distortion.

During the tie girder examination on November 1, 1984, it was observed that several backing bars had joints that were not groove welded,

as illustrated in Fig. 74. A crack-like indication can be seen in the paint film although no significant oxide can be observed. It was recommended that these locations be ground out to remove any cracks and prevent their subsequent extension.

The retrofit plates recommended in May 1984[5] can be seen installed between the bottom flanges of the floor beam and tie girder in Fig. 75. This condition violates the AWS Specification which requires that backing bars be continuous.

7. RECOMMENDATIONS

During the course of this study several recommendations were made that were implemented during 1984. These are summarized here for clarity and to provide a record. Other recommendations are also provided.

(1) The September 1983 web gap strain measurements indicated that crack growth had likely developed at the root of the backing bar into the girder web or at the web-flange intersection. It was recommended that the backing bar be removed at a diaphragm where significant growth had occurred in the diaphram-web welded connection. A bar was removed in October 1984. Inspection on November 1, 1984 verified that fatigue crack extension had developed at both of the suspected areas.

(2) It was recommended that a second set of strain measurements be acquired after the initial retrofit in order to assess the effectiveness of the bolted connections between the diaphragm and the top and bottom flanges. It was suggested that the angles alone would not be sufficient to reduce the interior web gap distortion at the floor beam connection. These measurements were acquired during the week of April 16, 1984.

(3) The April 1984 strain measurements verified that a more positive connection was needed between the bottom flange of the floor beams and the bottom flange of the tie girder. It was recommended that a bolted splice plate be installed to provide

such a connection. These plates were installed during the fall of 1984.

(4) Several backing bars in the tie girder were observed to be installed without a full fusion groove weld to provide continuity in the backing bar during the November 1, 1984 site visit. It was recommended that these locations be ground out and inspected to insure that transverse cracks did not extend into the box corner weld. This was carried out by the contractor in November 1984.

(5) It is recommended that the diaphragm-web connections that had specimens removed for examination of the crack surfaces and other locations which exhibited cracking be monitored during the normal two year inspection interval to determine whether or not any additional crack extension has developed at the drilled retrofit holes. The inspection reports provided in Ref. 3 can be used to identify these locations.

(6) A thorough inspection is needed of all box corners to insure that all locations with discontinuous backing bars have been identified and corrected. The lack of fusion areas need to be ground out and the backing shaped to minimize the stress concentration and remove any cracks or discontinuities. These locations should be given a careful examination during the regular two year inspection.

(7) In view of the detection of discontinuous backing bars in November 1984 during entry into only one floor beam - tie girder connection area, it is recommended that a careful inspection be carried out on the two tie girders by bridge inspectors with experience. Attention should be directed to all welded connections such as intersecting welds at diaphragm - horizontal stiffener connections, box corner welds at sealed diaphragms and other welded attachments.

8. SUMMARY AND CONCLUSIONS

The conclusions are the following:

(1) The strain measurements from random traffic demonstrated that significant cyclic stresses are introduced into the diaphragm-web welded connection and the tie girder web gaps as a result of the end restraint at the floor beam-tie girder connections.

(2) Fatigue crack growth was detected in all weld cracks examined. The rate of crack propagation was relatively high ($2\text{-}5 \times 10^{-6}$ in/cycle) which is not unusual for a random variable load history.

(3) The lack of fusion between the fillet weld roots of the diaphragm-web welded connection promoted crack extension under repeated loads.

(4) From the observed initial lack of fusion condition that existed at the ends of the diaphragms and seen in the samples, the crack growth threshold would be exceeded by a stress range of 1.5 or 3 ksi.

(5) The striation spacing observed on the crack surface of the samples removed from T1A-NB top and T2A-NB top indicated that the crack growth rate was relatively high.

(6) All cracks in the diaphragm-web weld connections were in a plane that is parallel to the primary stresses in the tie girder. These cracks did not affect the strength and integrity of the structure.

(7) The structure can remain in service to traffic prior to carrying out corrective action. (Retrofitting was carried out in 1984 so that crack growth is minimized.)

(8) The web gap strain measurements demonstrated that high out-of-plane web bending stresses are introduced into the web. These cyclic stresses are particularly high when projected to the weld at the root of the backing bar. Hence, cracking can develop at the root in the web flange weld as a result of these stress cycles. All four box corners would be susceptible.

(9) These cracks will be parallel to the primary stresses in the tie girder and do not affect its resistance. Examination of the root area after several backup bars were removed confirmed that crack extension had developed from the lack of fusion planes of the backing bar.

(10) The initial retrofit procedure which involved connecting the interior diaphragm to the top and bottom flange was not found to be adequate at the bottom inside corner adjacent to the floor beam. Strain measurements showed no significant

reduction at the bottom inside corner, whereas elsewhere the web gap distortion stresses were less than 1 ksi.

(11) The undesirable condition at the bottom inside corner was eliminated by installation of a flange splice plate (see Fig. 75). These plates were installed during the fall of 1984.

The retrofits implemented on the I79 tie girders will prevent further crack extension and should be effective for throughout the life of the structure. Any cracking in the box corner welds as a result of the prior history of distortion is not significant. The I79 bridge will not have its safety or future performance affected by the tie girder box corners at diaphragms nor the welded connections between the diaphragms and tie girder webs. The remaining life of this structure will not be affected by these conditions.

REFERENCES

1. Letter to B. F. Kotalik, Chief Bridge Engineer from R. E. Currier, District 11 Engineer, dated September 12, 1983.

2. Letter to L. M. Papet, Division Administrator, FHWA from B. F. Kotalik, Chief Bridge Engineer, dated September 23, 1983.

3. Magnaflux Quality Services
   Magnetic Particle Examination of I79 Bridge Sections at Neville Island, February 7, 13, and 14, 1984; April 2, 1984.

4. Fisher, J. W.
   FATIGUE AND FRACTURE IN STEEL BRIDGES, John Wiley and Sons, 1984.

5. Letter to H. P. Koretzky from J. W. Fisher, dated May 15, 1984.

TABLE 1

LOCATION AND TYPE OF VEHICLES ON BRIDGE DURING MEASUREMENTS*

Record No.	Northbound			Southbound		
	Lane 1	Lane 2	Lane 3	Lane 1	Lane 2	Lane 3
1		3S2				
2				57	3S2	
3		3S2				
4		3S2		2S3 3S2		72
5		3S2 3S2		3S3		
6		3S2		3S2		3S2
7					2S2 3S2	
8	3S2					
9						3S2
10		4D	3S2			
11		3S2 3S2	4D			
12		3S2				
13		3S2 3S2			2S2 3D 2S1	
14	-3S2 3S2				3S2	
15	2D					
16			3S2			
17	3S2	3S2		2S2		
18		3S2				
19		2S2 2S2	3S2	3S2 3S2		
20	3S2					
21		3S2				
22	3D					
23		3S2				
24					3S2	3S2
25				3S2		3S2
26		3S2			3S2	
27		3S2 3S2 3S2	3S2	3S2 2S2 3S2	3S2 3D 3S2	3S2
28	3S2	3S2 3S2		3S2		
29	3S2	3S2	3S2 3S2	3S2		3D

*No vehicle weights were obtained

TABLE 2

TYPICAL STRESSES IN DIAPHRAGM AND IN WEB GAPS*

- FALL 1983, PRIOR TO RETROFIT

(a) Diaphragm Stress Normal to Web

Panel Point	Top Outside	Bottom Outside
13	5.3 ksi	1.5 ksi
14	5.6 ksi	2.3 ksi

(b) Extrapolated Web Gap Stress

Panel Point	Top Outside Web		Top Inside Web	
	End of Diaphragm	Root of Backing Bar	End of Diaphragm	Root of Backing Bar
13	12 ksi	18 ksi	4.5 ksi	8 ksi
14	2 ksi	16 ksi	1 ksi	20 ksi
	Bottom Outside Web		Bottom Inside Web	
13	4 ksi	3.4 ksi	5 ksi	8.5 ksi
14	3.5 ksi	7.5 ksi	1 ksi	17 ksi

*Observed under random truck traffic.
No vehicle weights were obtained.

TABLE 3: I79 AFTER RETROFIT

Gage		Stress Range (ksi)
73R	Top Floor Beam Flange, PP14	1.9
74R	Inside Web, PP14	1.8
74W	Inside Web, PP14	2.7
75R	Inside Web, PP14	4.5
75W	Outside Web, PP14	≃0.3
76R	Outside Web, PP14	≃0
76W	Outside Web, PP14	≃0
77R	Bottom Floor Beam Flange, PP14	0.7
78W	Outside Web Face, PP14	1.4
78R	Outside Web Face, PP14	1.3
79W	Outside Web Face, PP14	1.5
79R	Outside Web Face, PP14	1.3
80R	Outside Web Face, PP14	≃0.4
71W	Around Core, PP14	1.8
71R	Around Core, PP14	1.5
72W	Around Core, PP14	1.0
72R	Around Core, PP14	5.0
81WV	Outside Web Face, PP13	3.2
81WH	Outside Web Face, PP13	1.1
82W	Outside Web Face, PP13	1.1
82R	Outside Web Face, PP13	1.0
83W	Outside Web Face, PP13	0.9
83R	Outside Web Face, PP13	1.2
84R	Outside Web Face, PP13	1.1

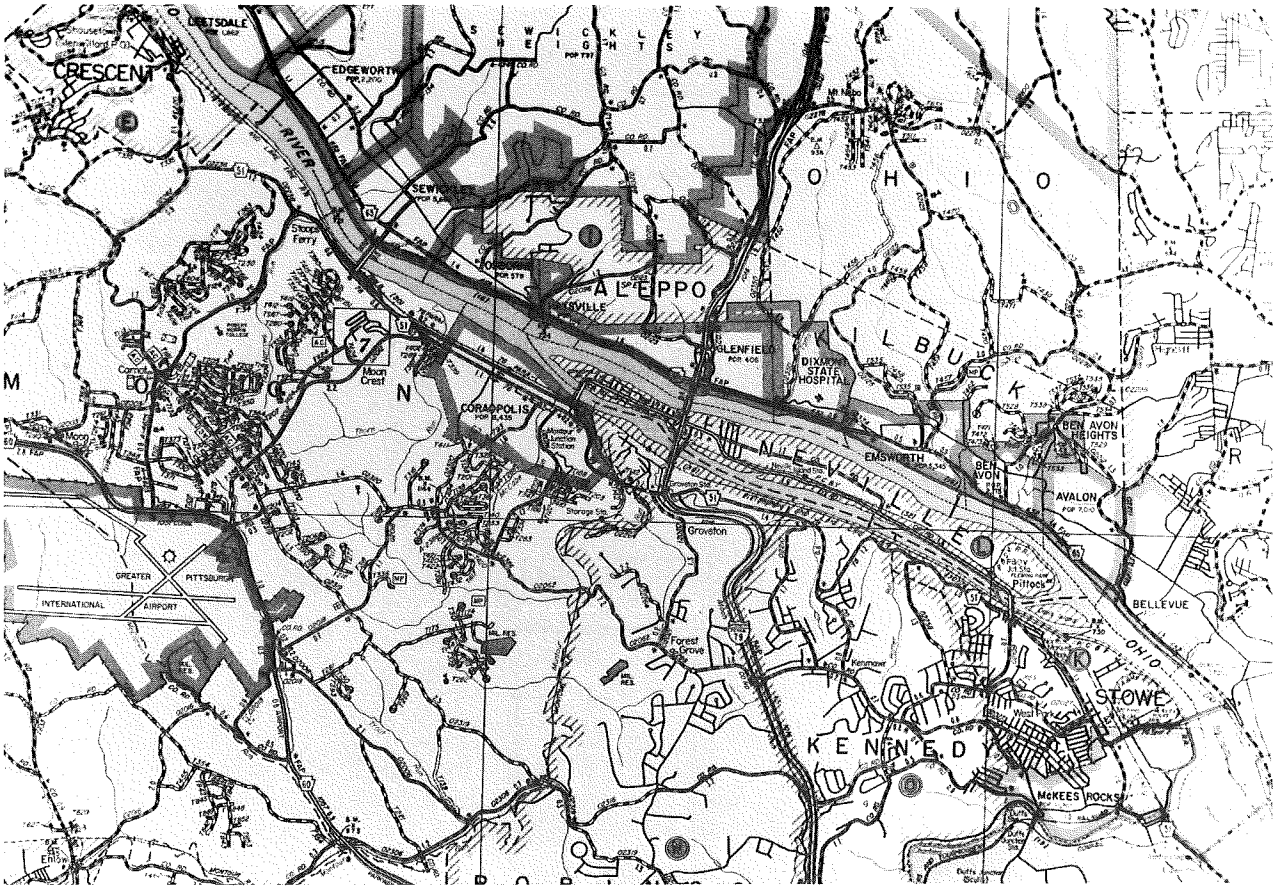

Fig. 1a Location Map Showing I79 River Crossing at Neville Island

Fig. 1b Elevation of the I79 Tied Arch Span

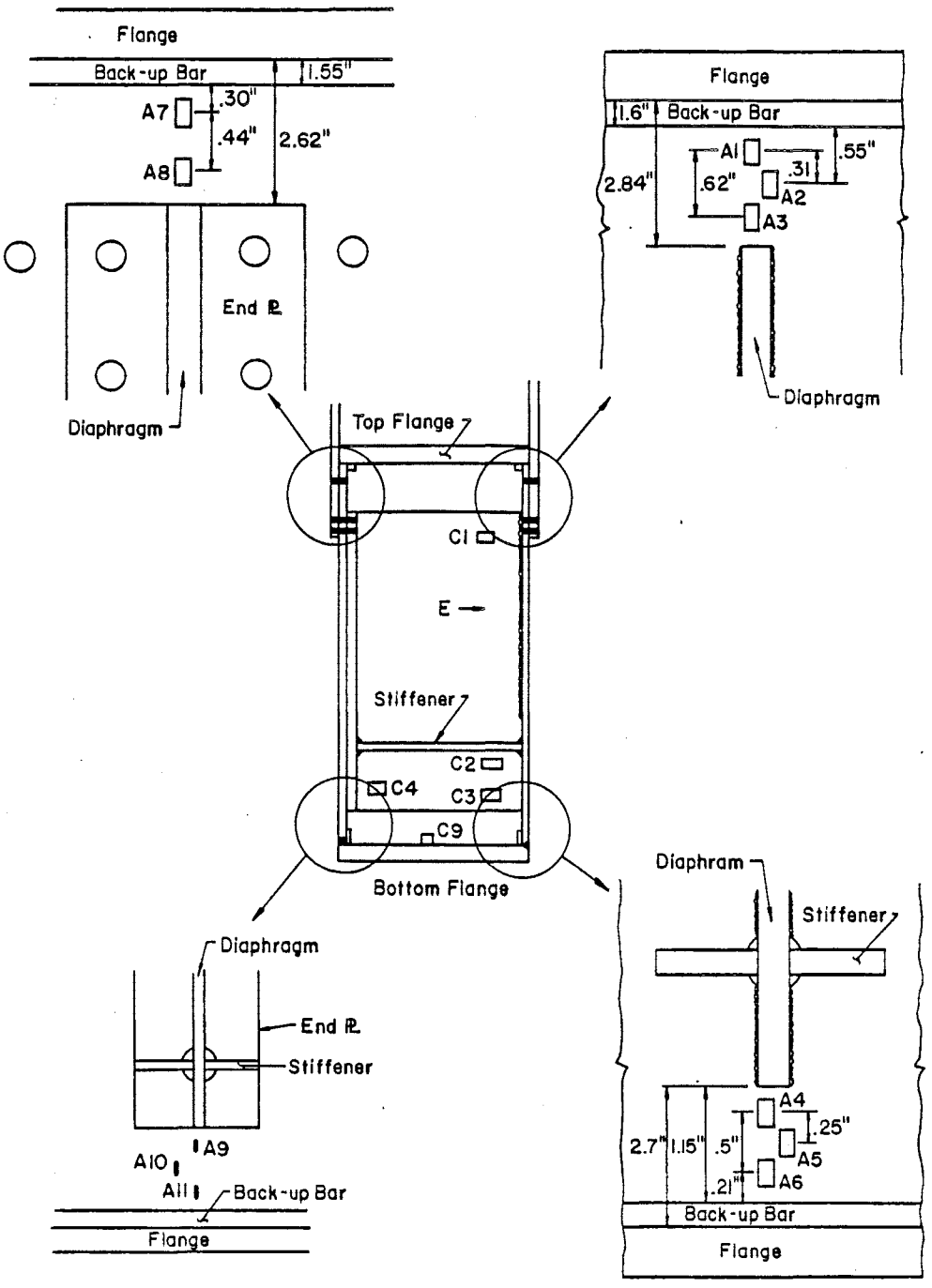

Fig. 2 Instrumentation Installed at Panel Point 13

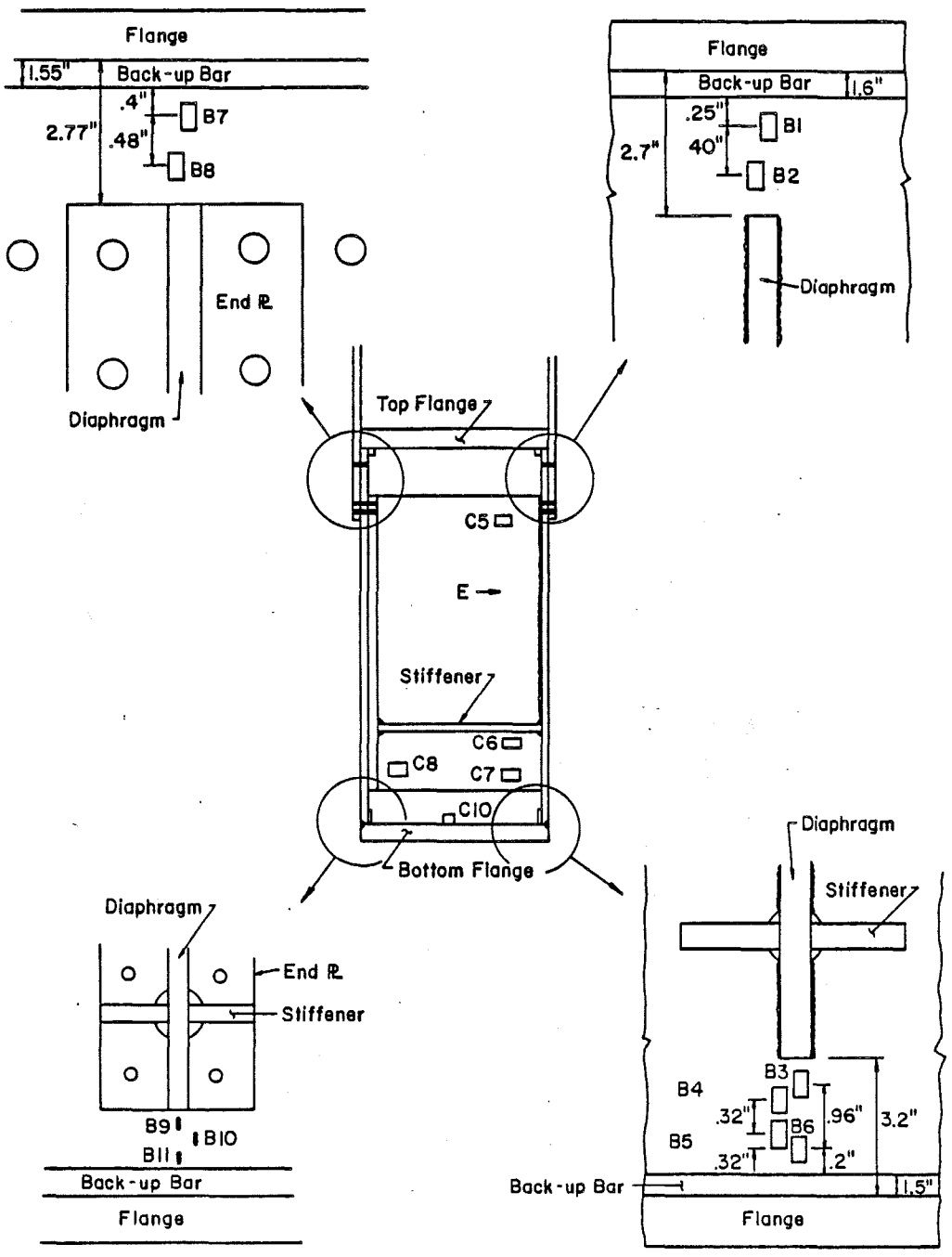

Fig. 3 Instrumentation Installed at Panel Point 14

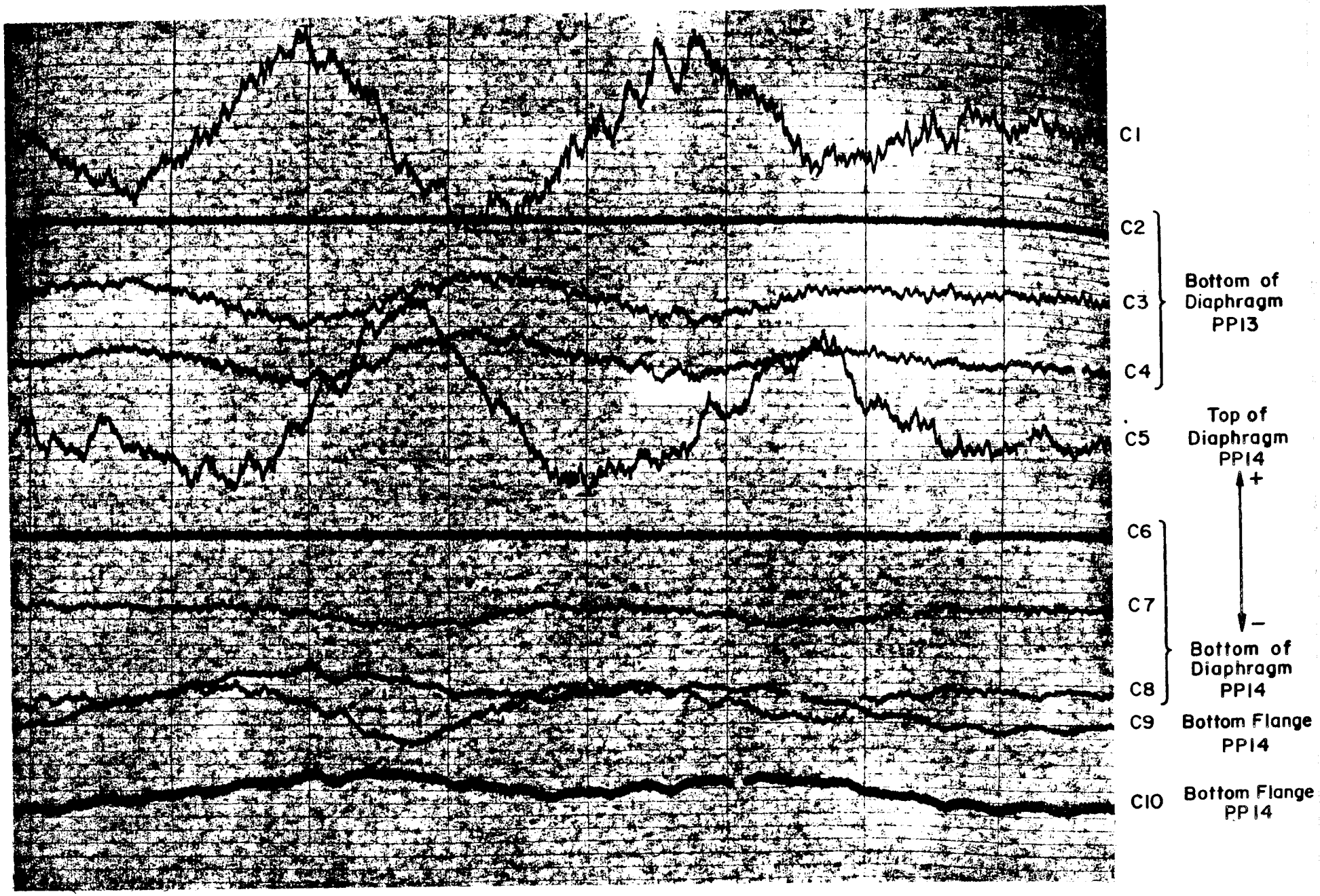

Fig. 4 Typical Time-Strain Response at Panel Points 13 and 14

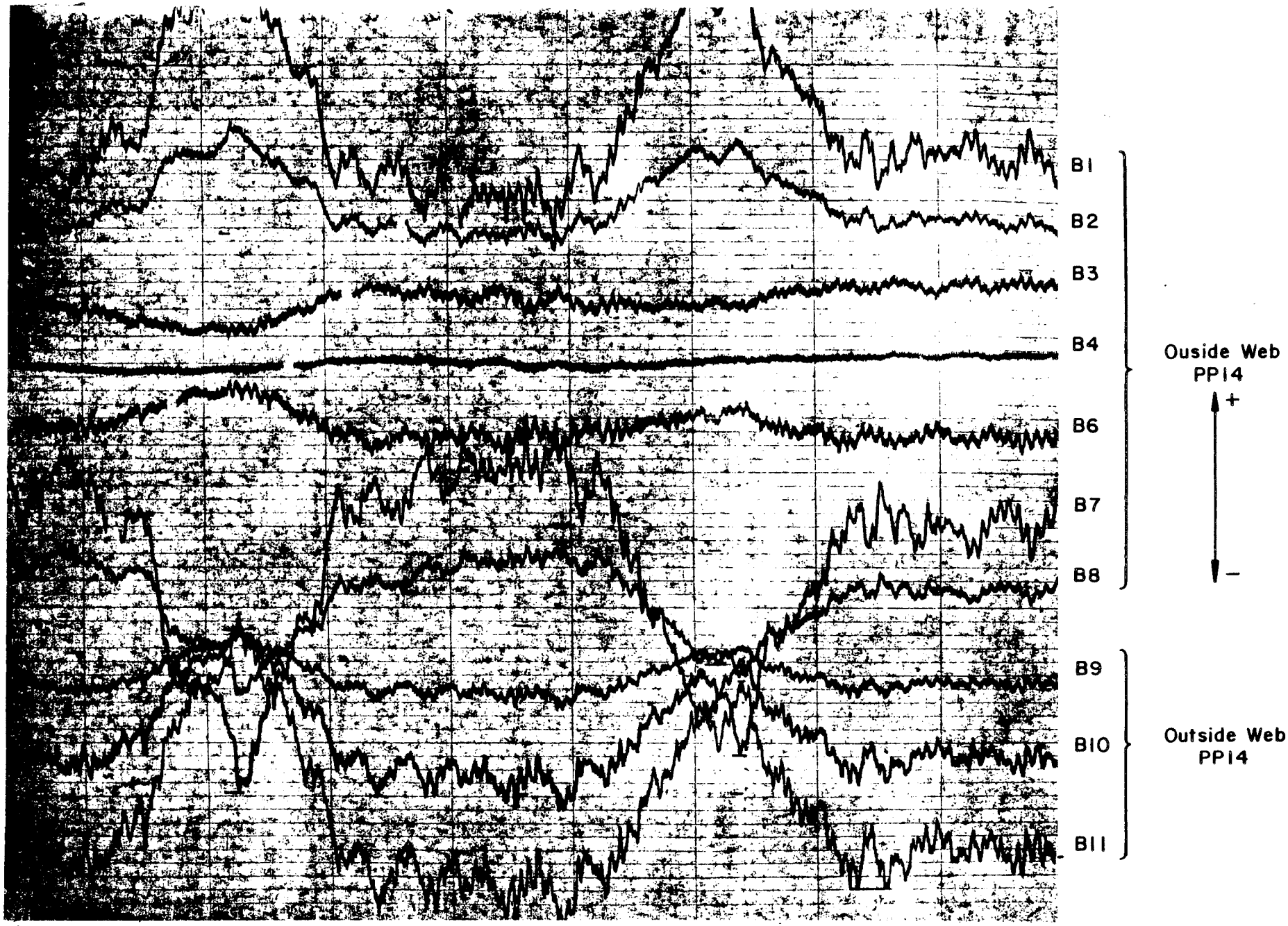

Fig. 5 Typical Strain Responses Observed at Panel Point 14

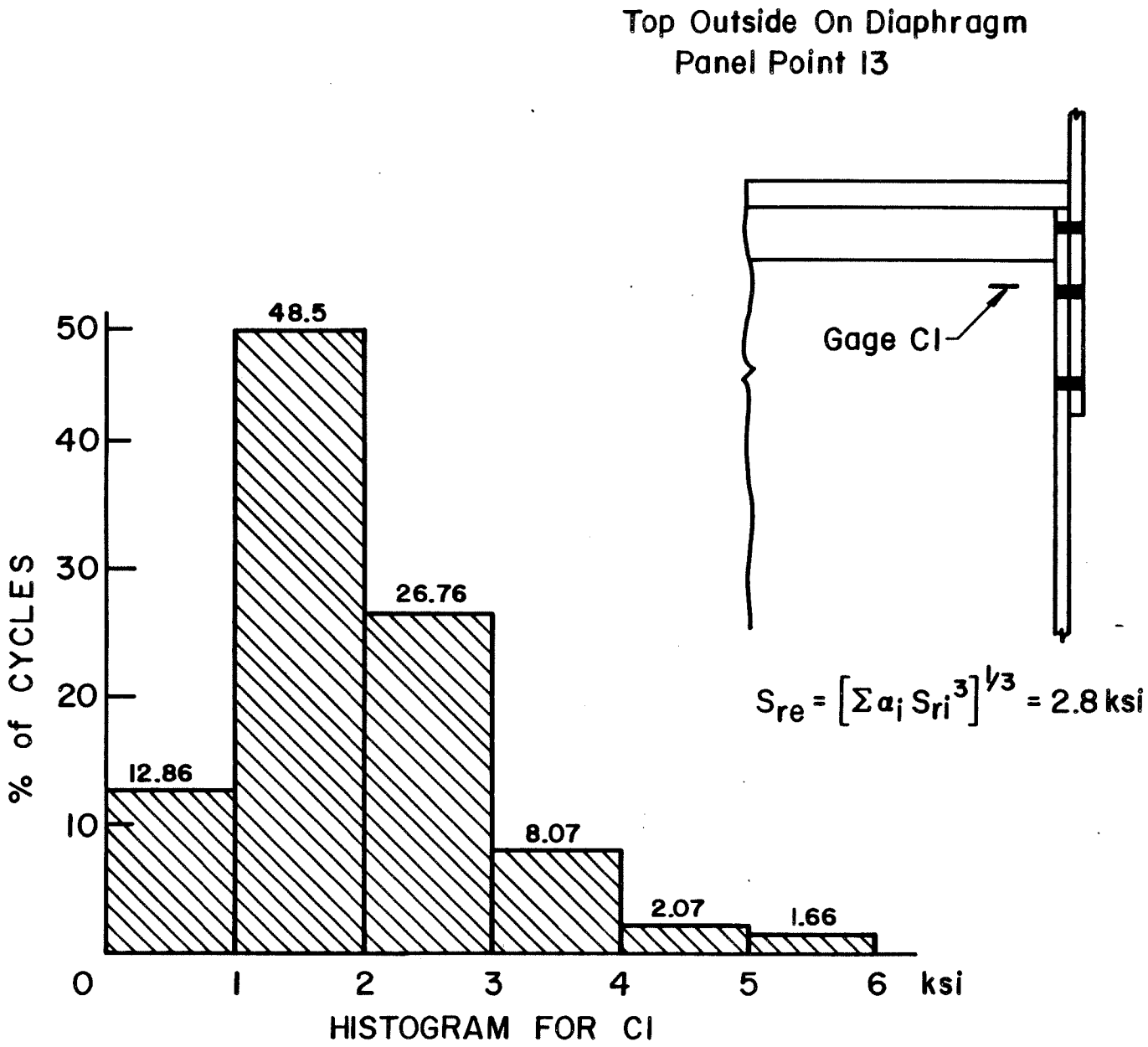

Fig. 6 Stress Range Histogram for Diaphragm at Panel Point 13

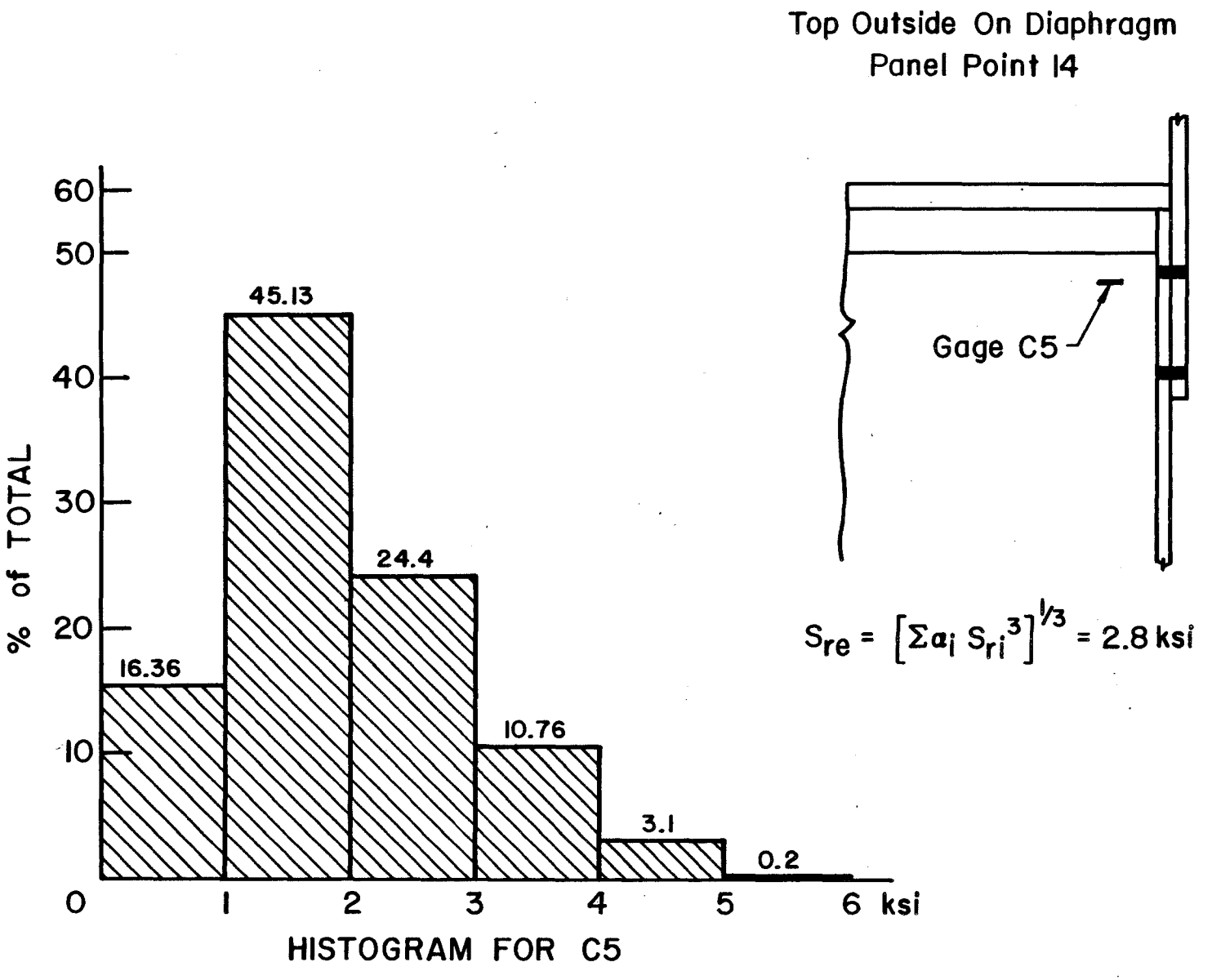

Fig. 7 Stress Range Histogram for Diaphragm at Panel Point 14

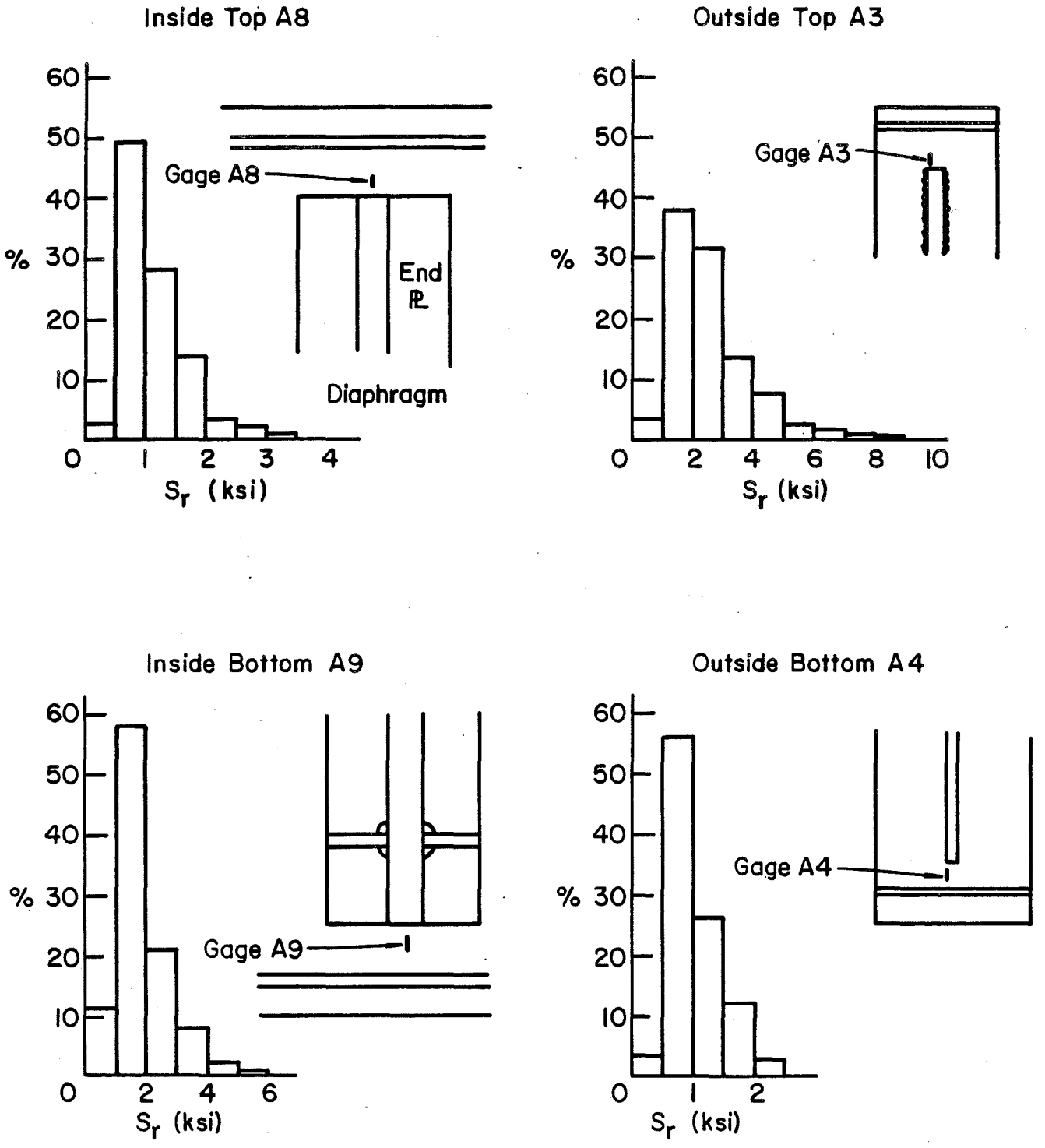

Fig. 8 Stress Range Histogram for Web Gaps at Panel Point 13

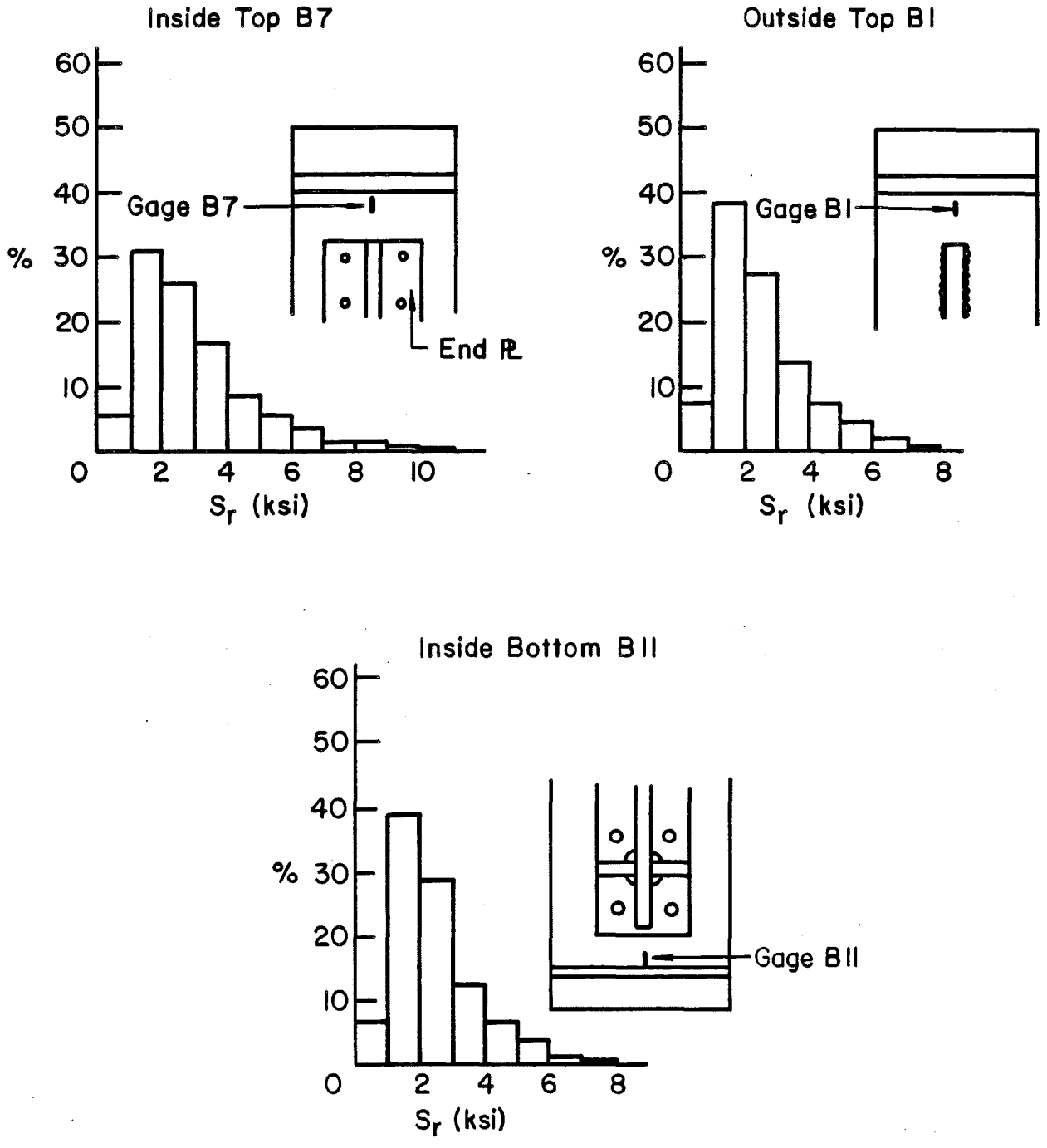

Fig. 9 Stress Range Histograms for Web Gaps at Panel Point 14

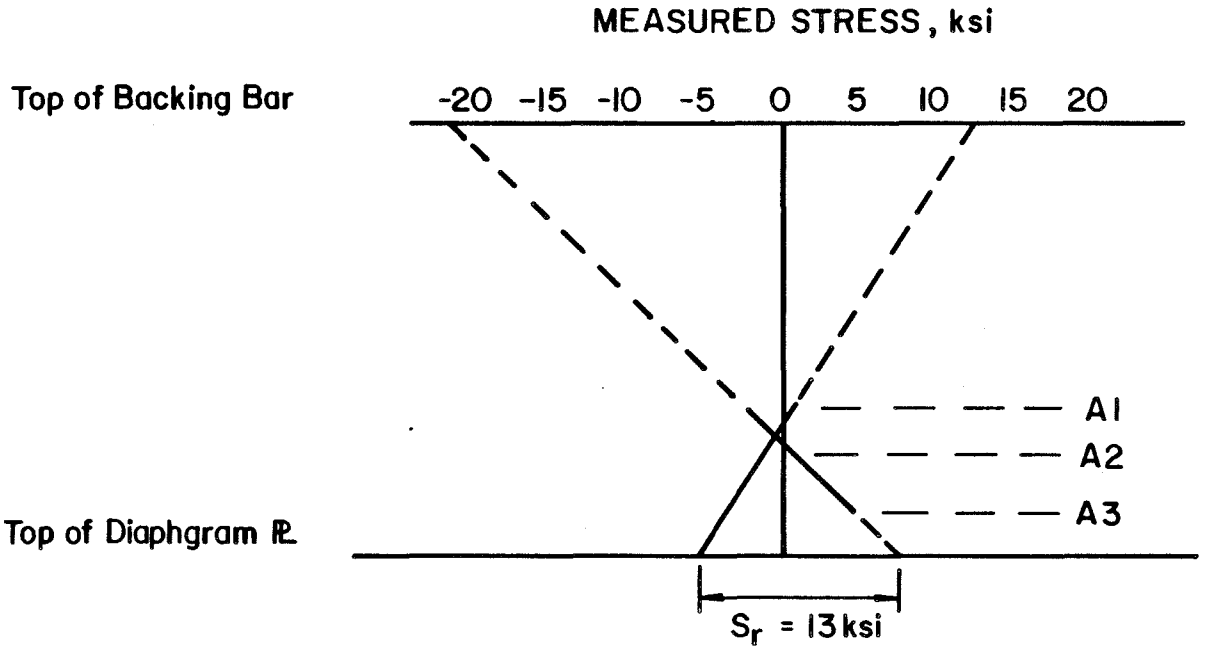

Fig. 10 Stress Gradient Observed at Top Outside Web Gap at Panel Point 13

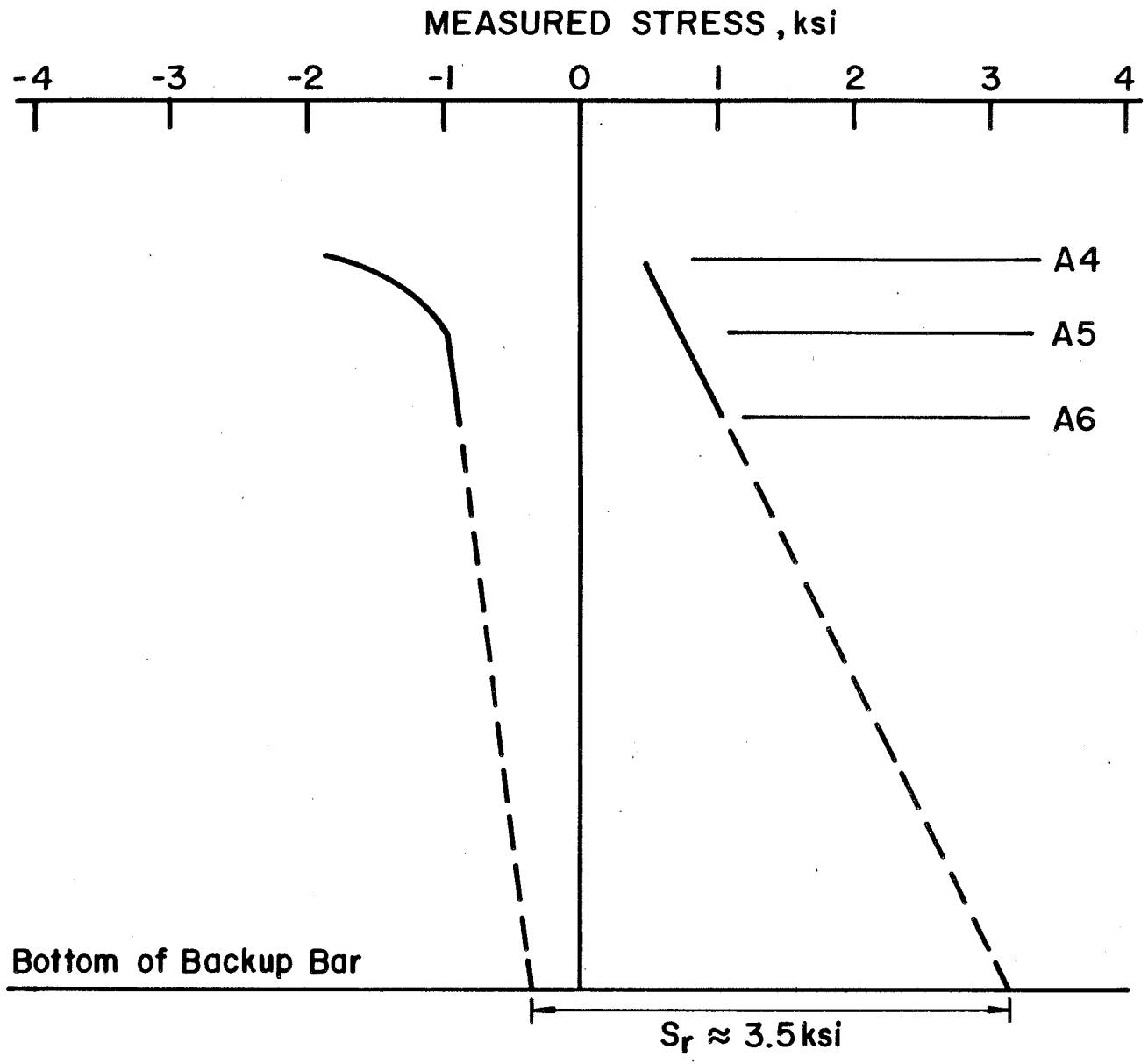

Fig. 11 Stress Gradients at Bottom Outside Web Gap at Panel Point 13

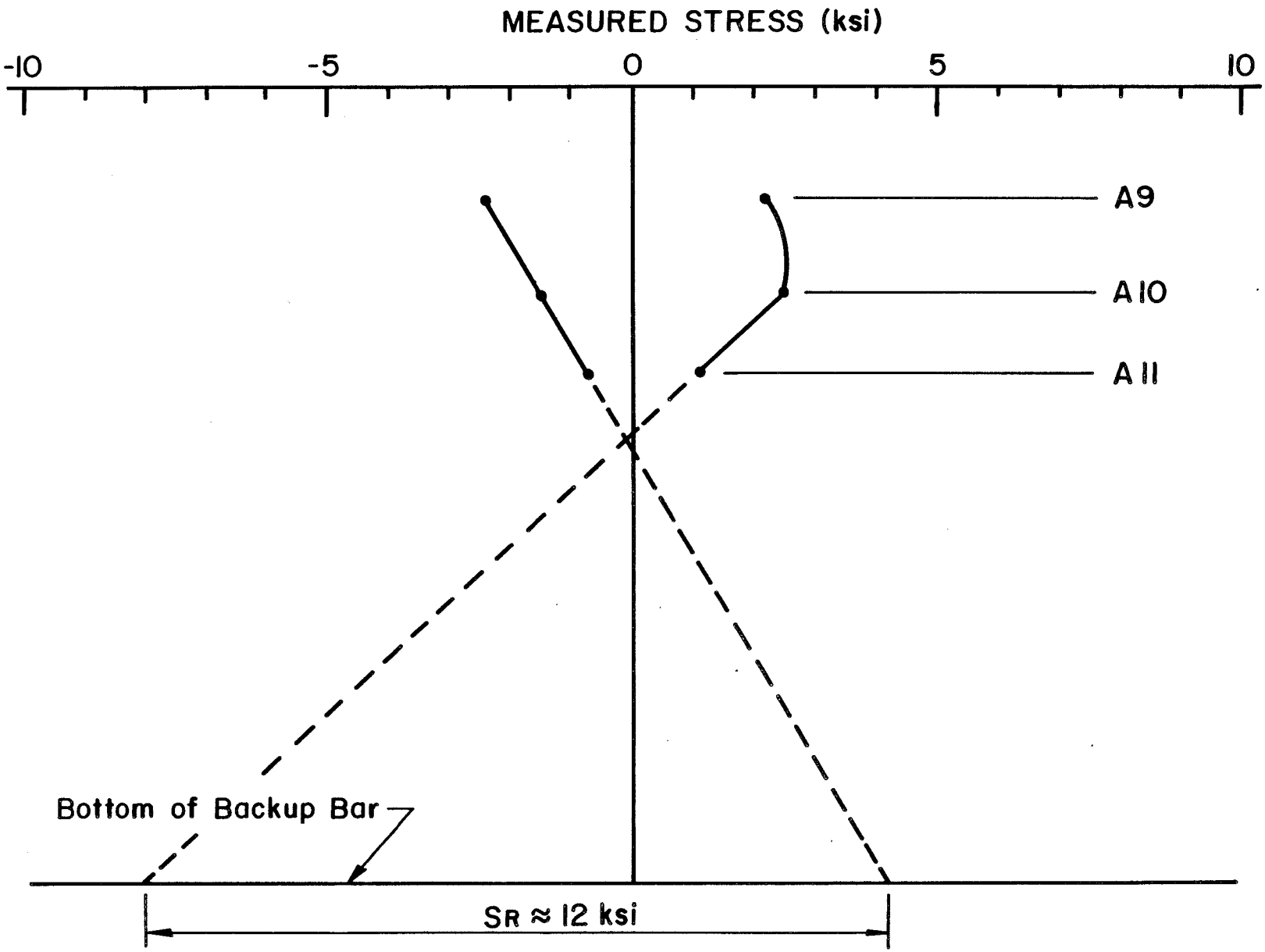

Fig. 12 Stress Gradients at Bottom Inside Web Gap at Panel Point 13

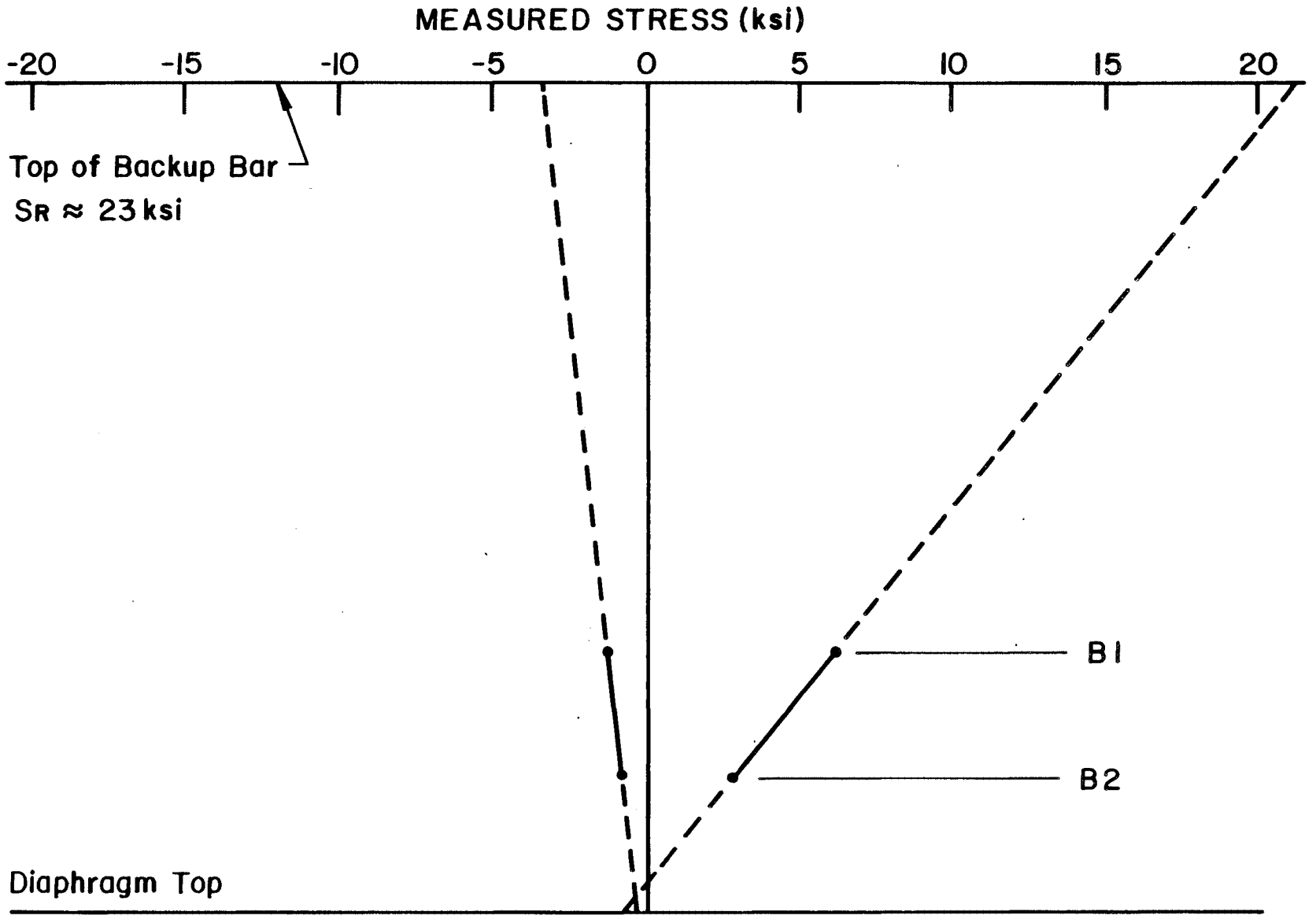

Fig. 13 Stress Gradients at Top Outside Web Gap Panel Point 14

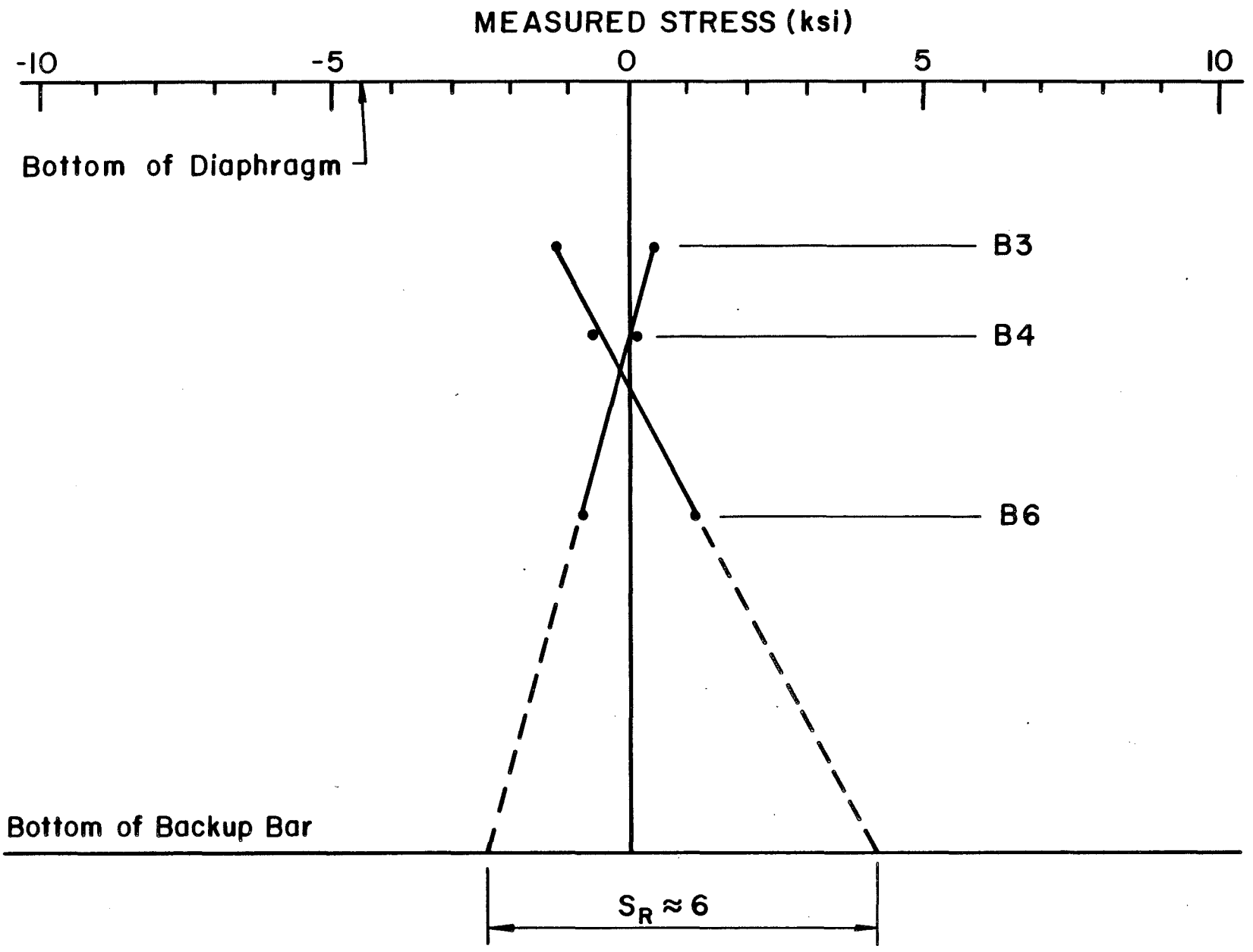

Fig. 14 Stress Gradients at Bottom Outside Web Gap - Panel Point 14

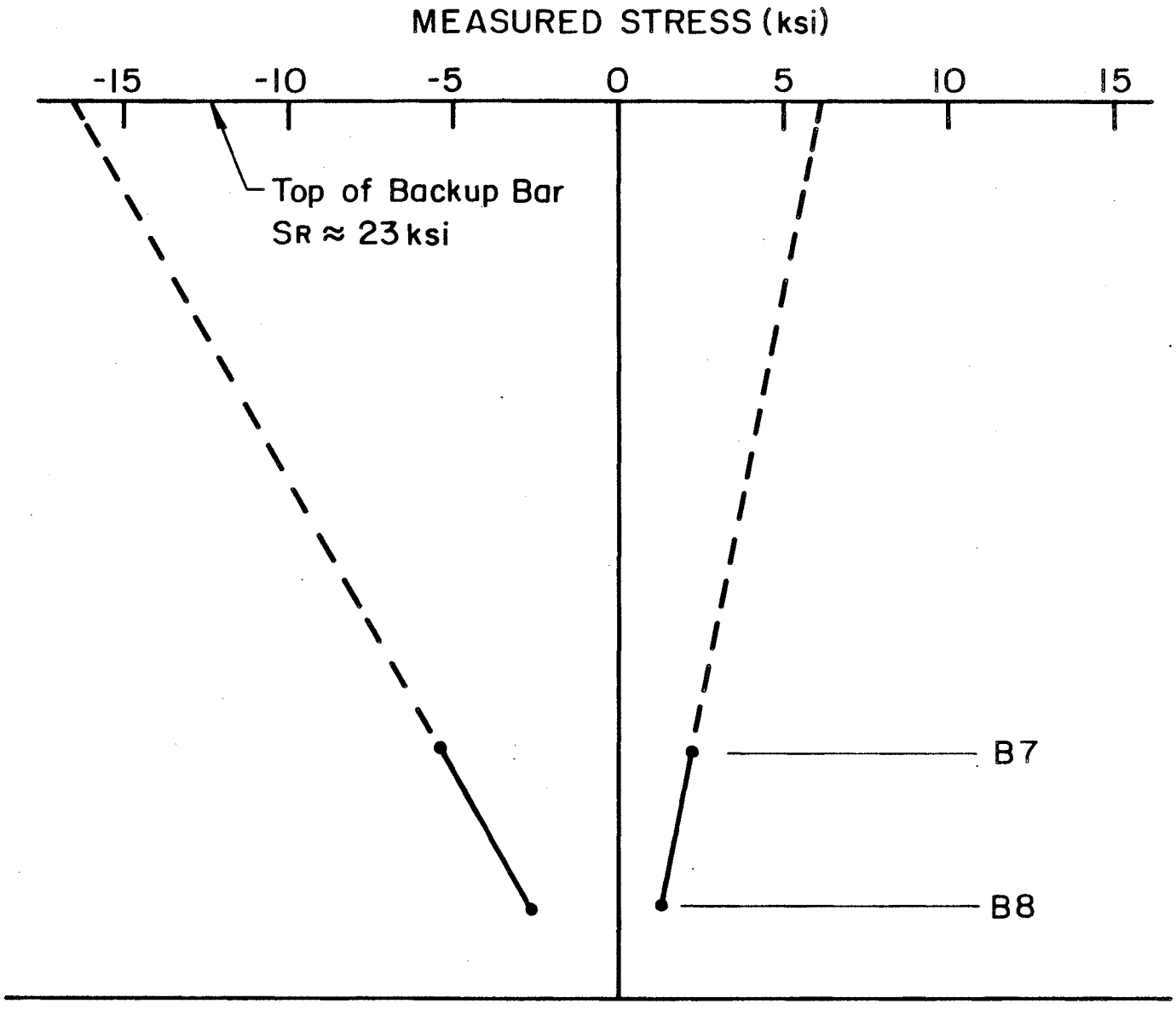

Fig. 15 Stress Gradients at Top Inside Web Gap at Panel Point 14

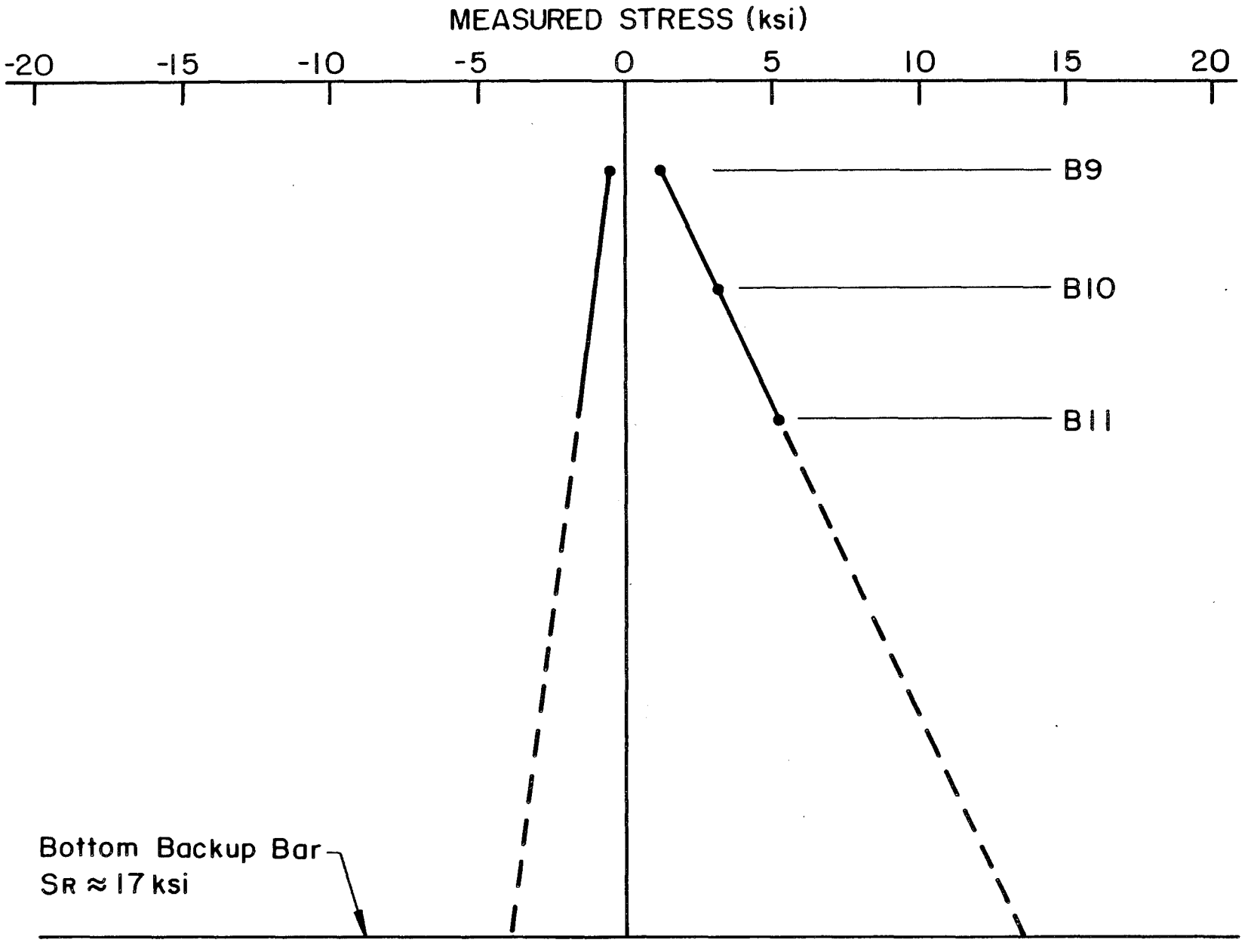

Fig. 16 Stress Gradients at Bottom Inside Web Gap at Panel Point 14

Run 18
B Gages

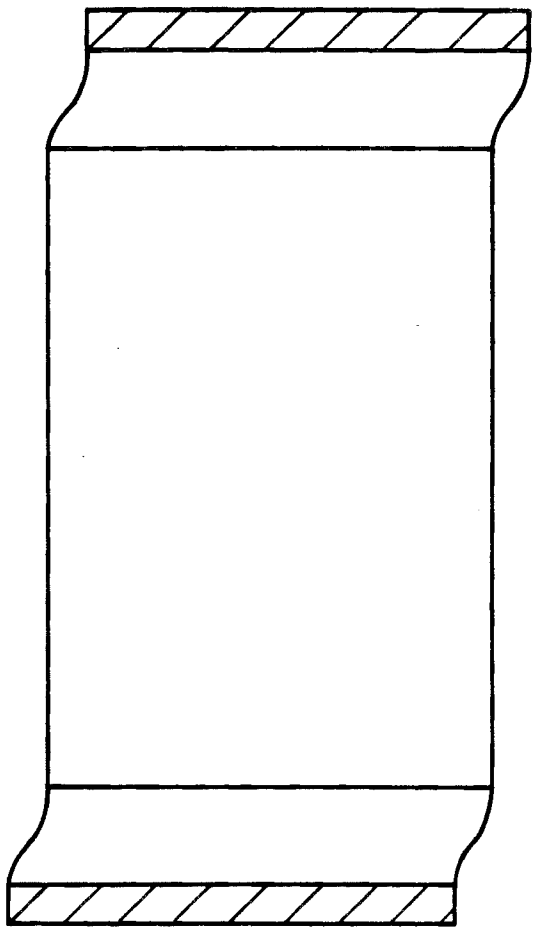

Time: T

Fig. 17 Schematic of Distorted Cross-Section at Time T

Run 18
B Gages

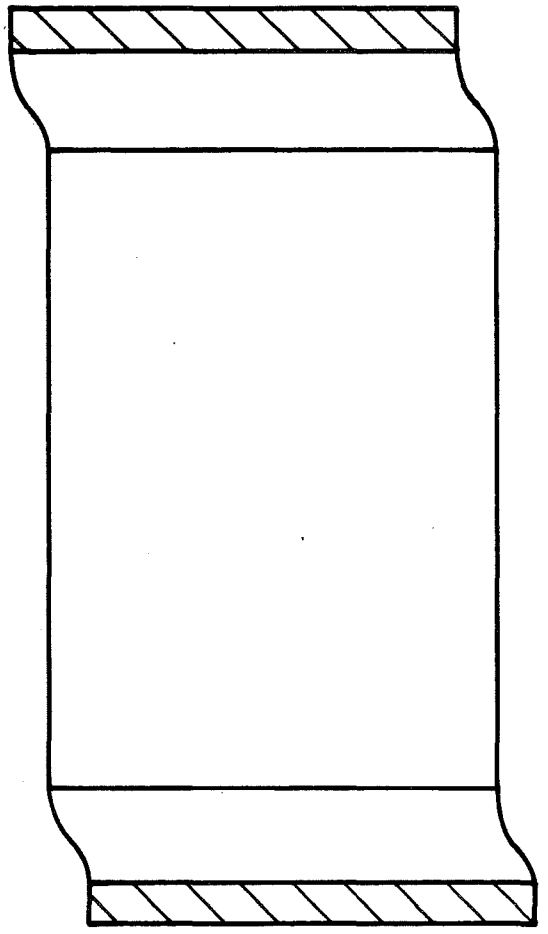

Fig. 18 Schematic of Distorted Cross-Section at Time T + t

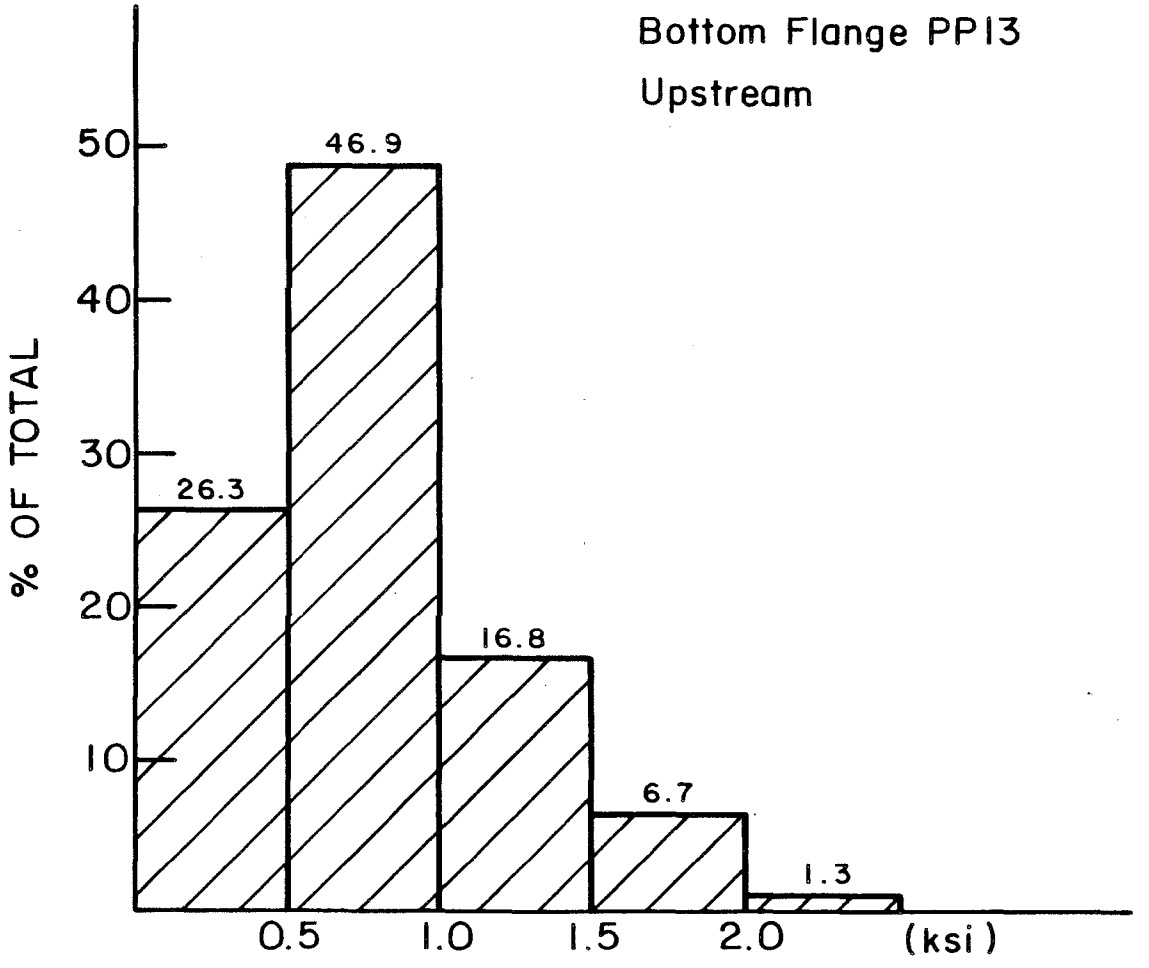

Fig. 19 Stress Range Histogram for Bottom Flange of Tie Girder at Panel Point 13U

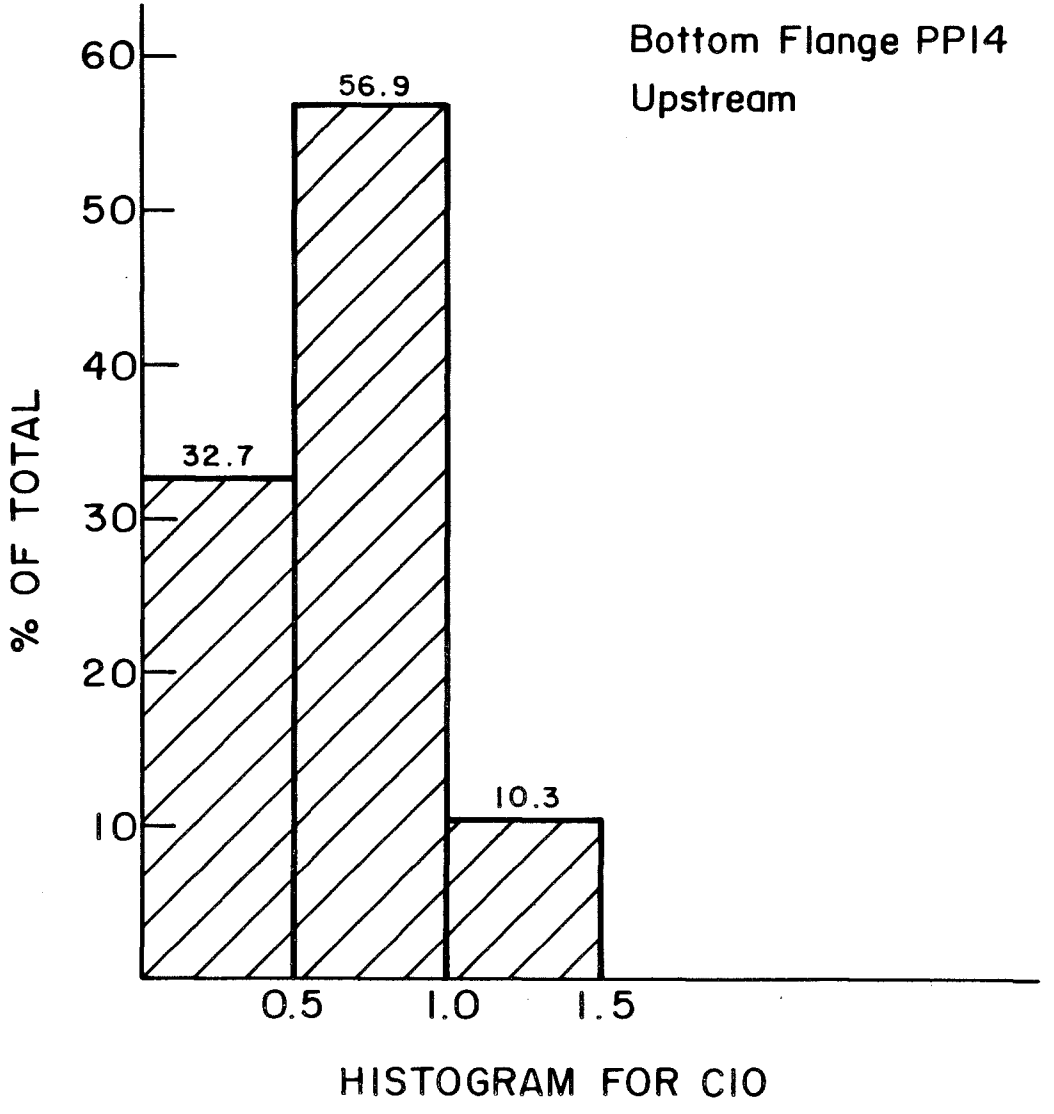

Fig. 20 Stress Range Histogram for Bottom Flange of Tie Girder at Panel Point 14U

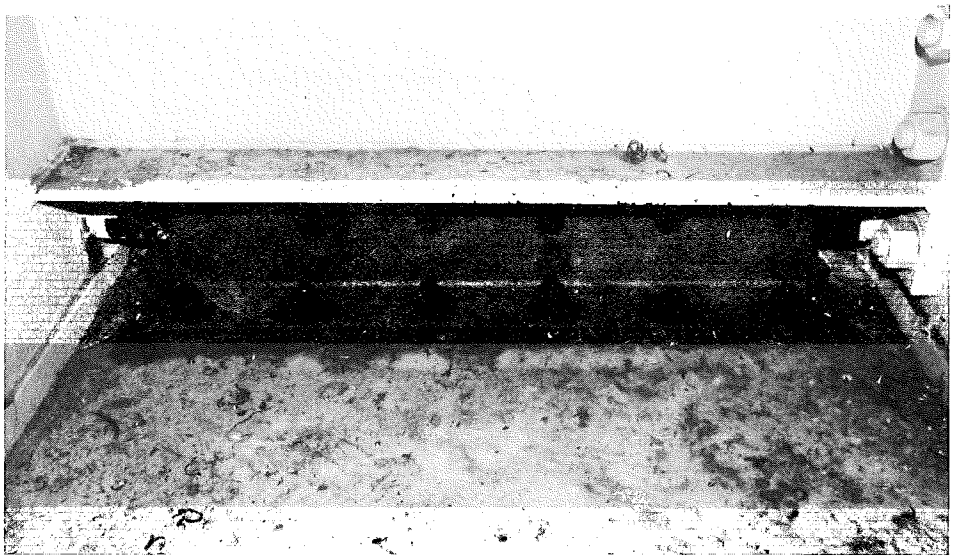

Fig. 21 Initial Retrofit Angles Attached to Diaphragm and Bottom Flange

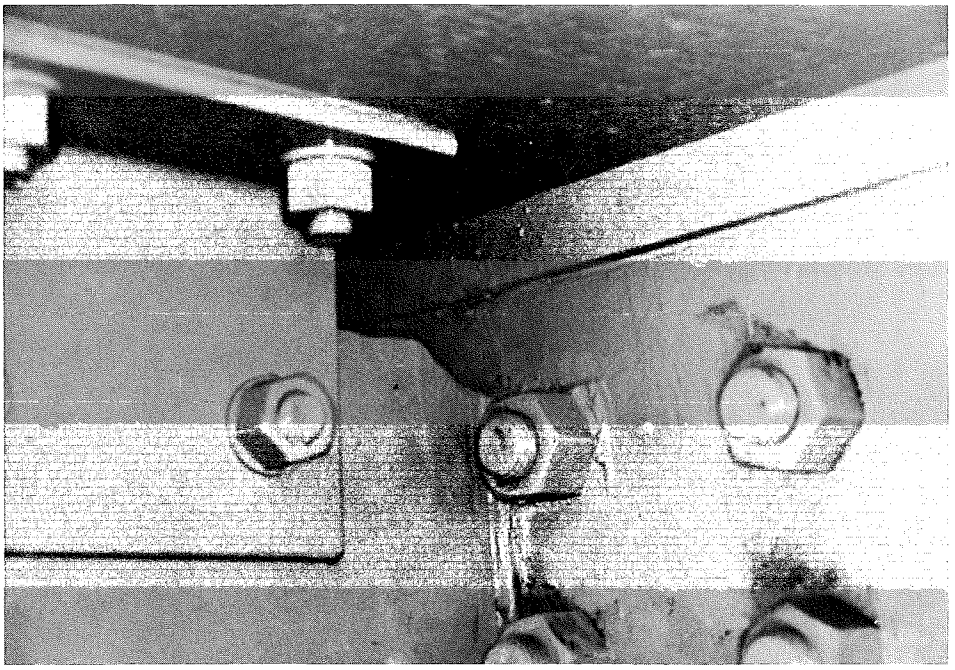

Fig. 22 Close-up of Upper Outside Gap Showing Retrofit Angle and Region of Diaphragm Where Crack Was Removed

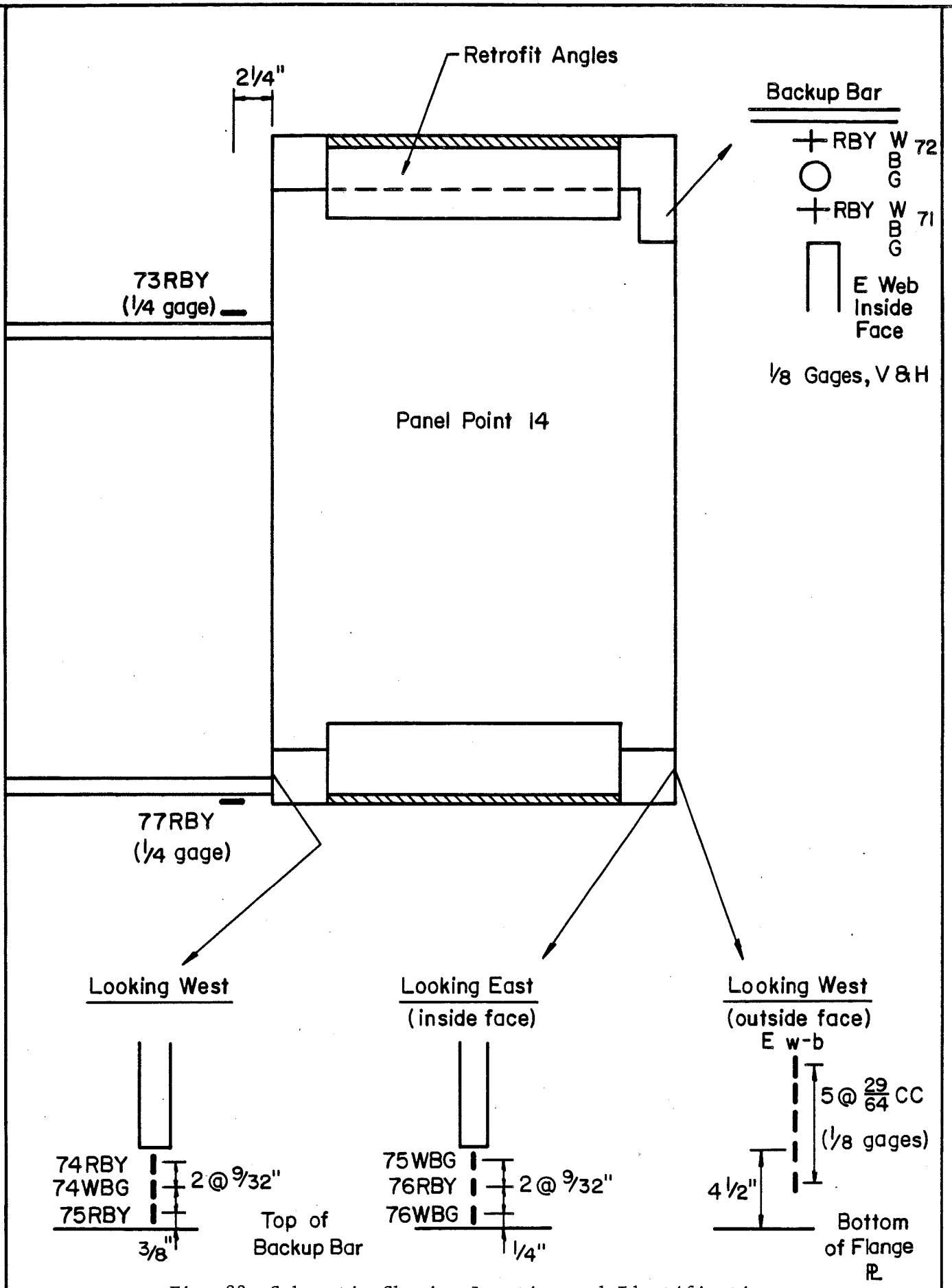

Fig. 23 Schematic Showing Location and Identification of Strain Gages at Panel Point 14

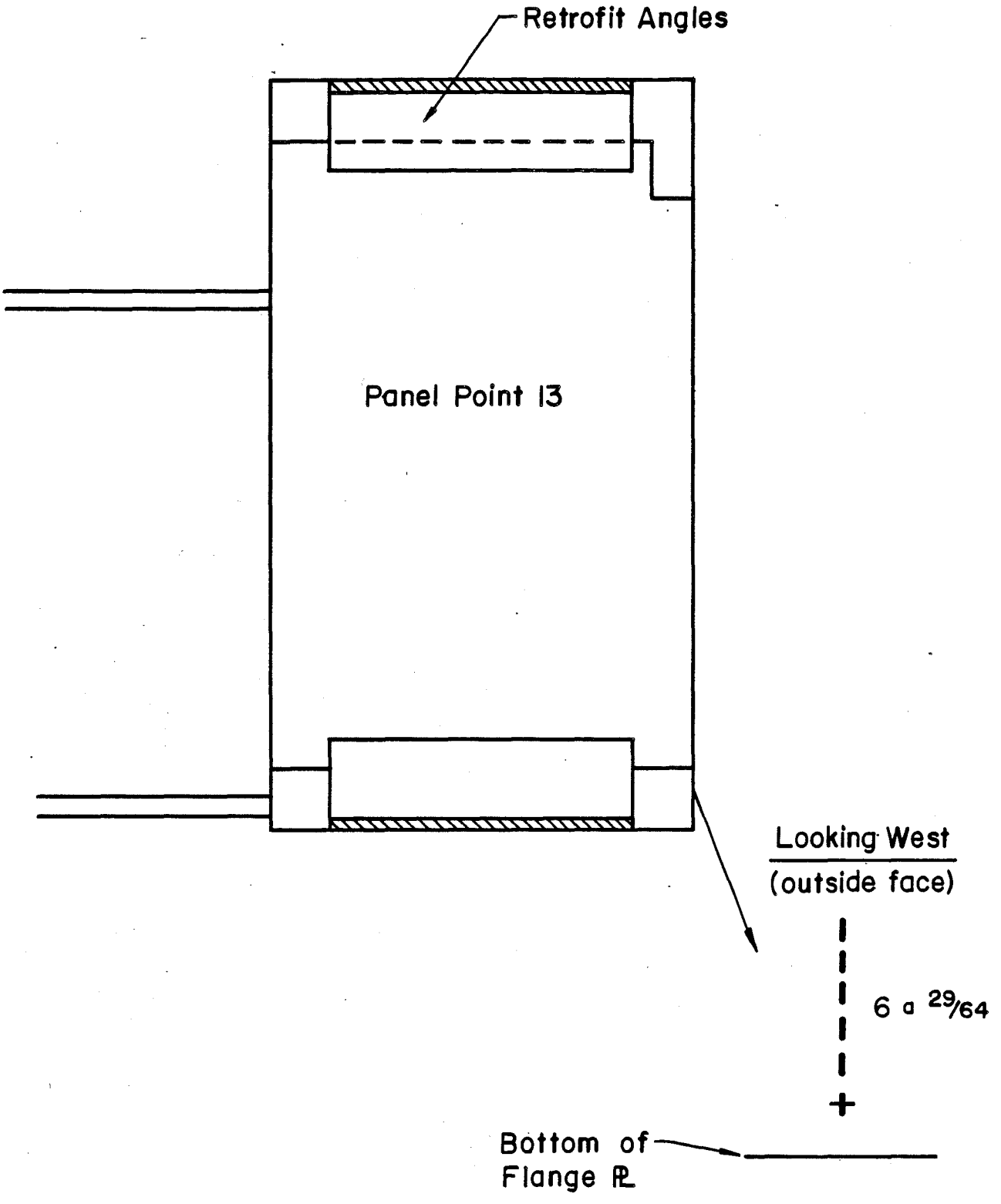

Fig. 24 Schematic Showing Location of Strain Gages at Panel Point 13

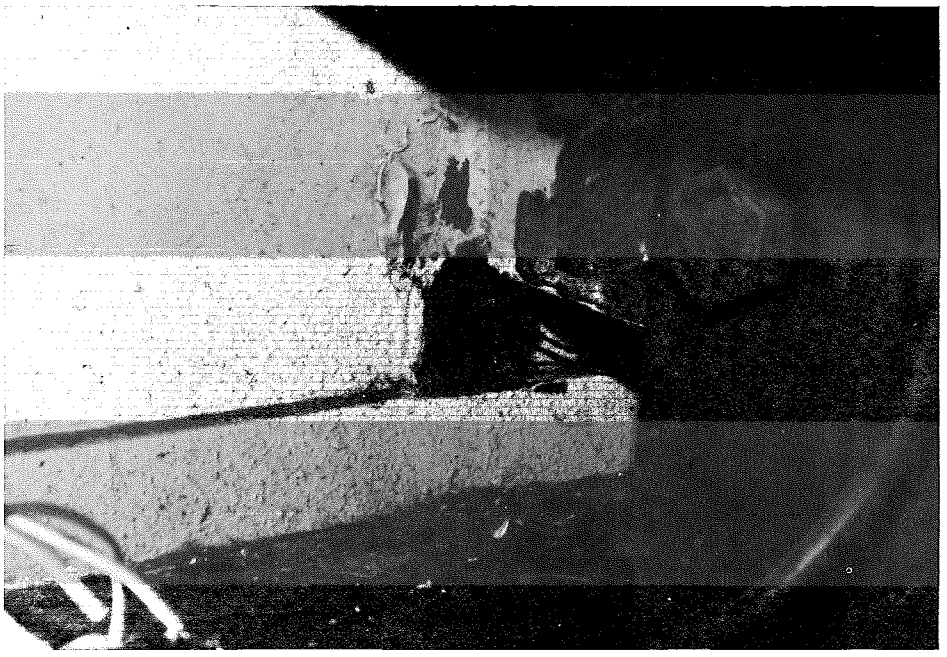

Fig. 25 Strain Gages Installed in Bottom Outside Web Gap

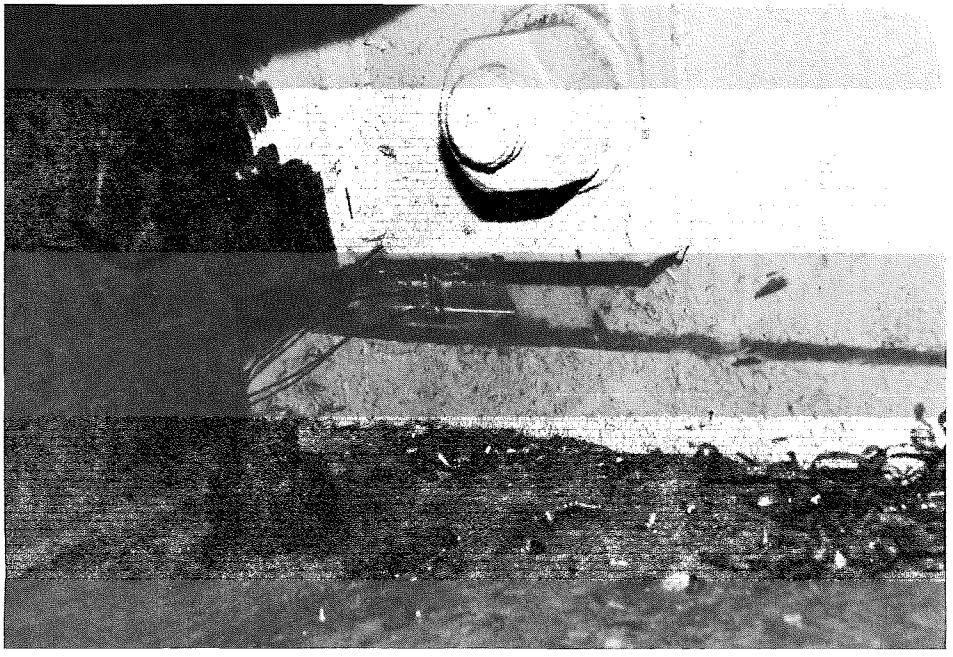

Fig. 26 Strain Gages Installed in Bottom Inside Web Gap

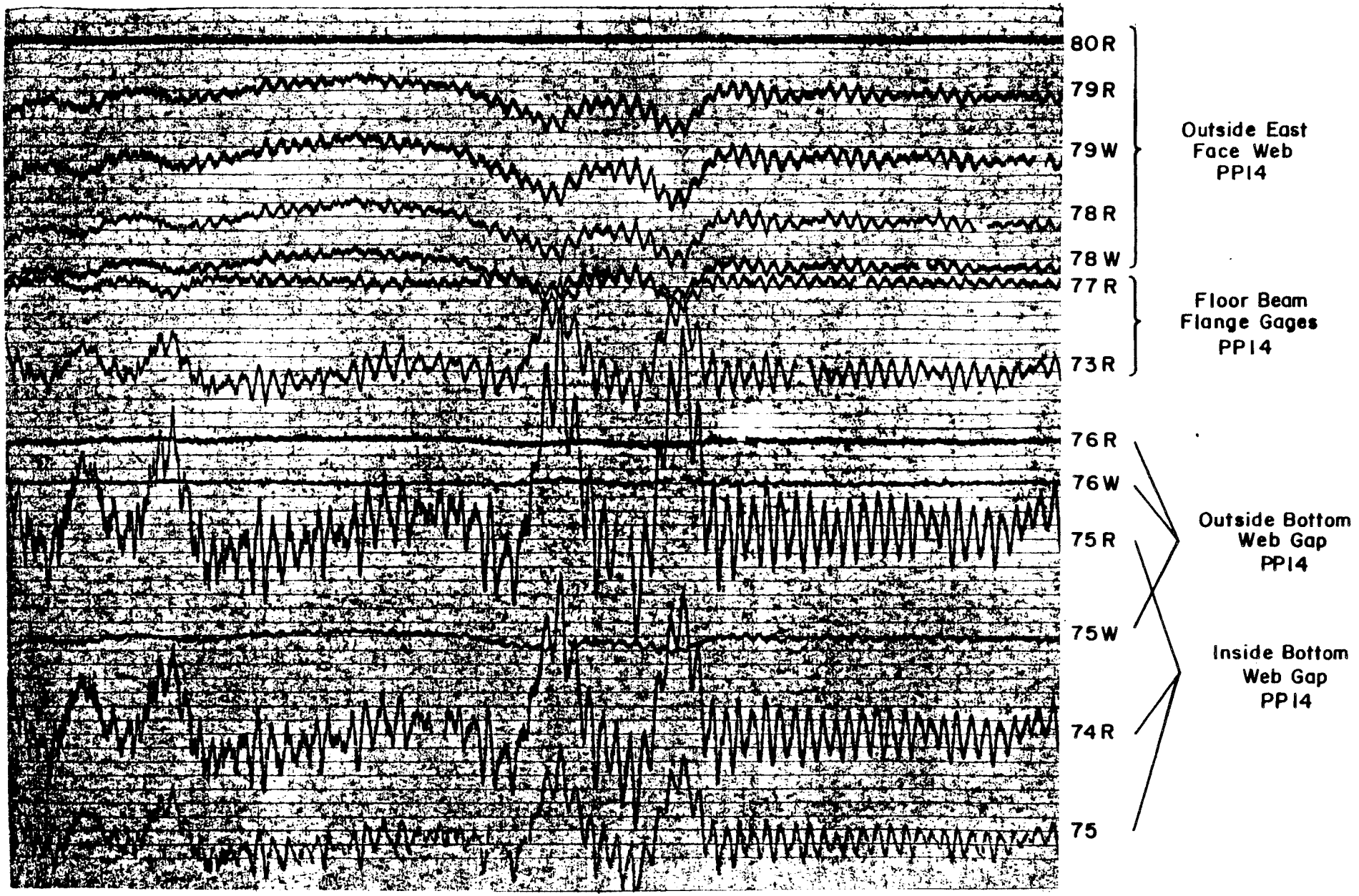

Fig. 27 Strain-Time Response at Panel Point 14

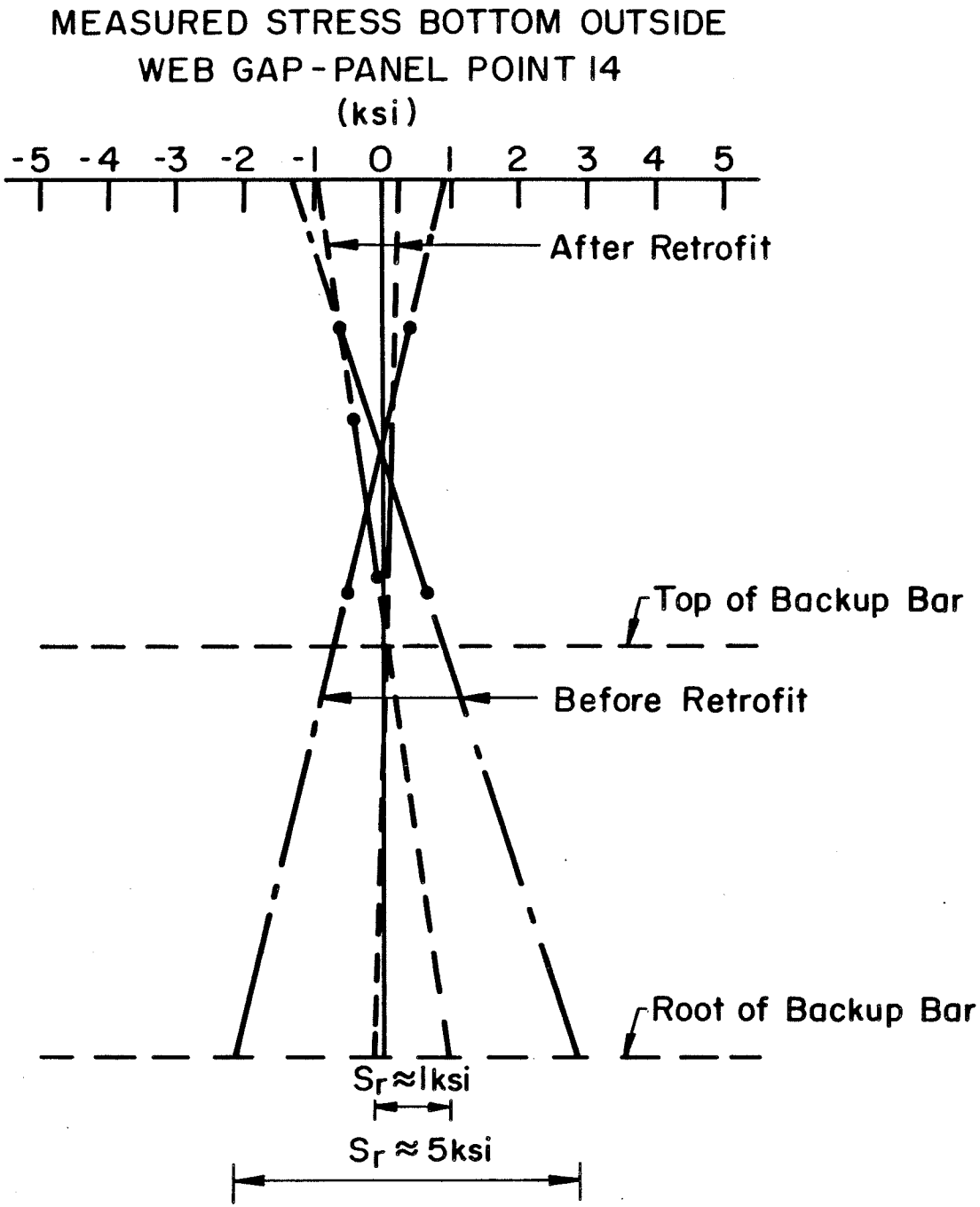

Fig. 28 Stress Gradient in the Bottom Outside Web Gap - Panel Point 14

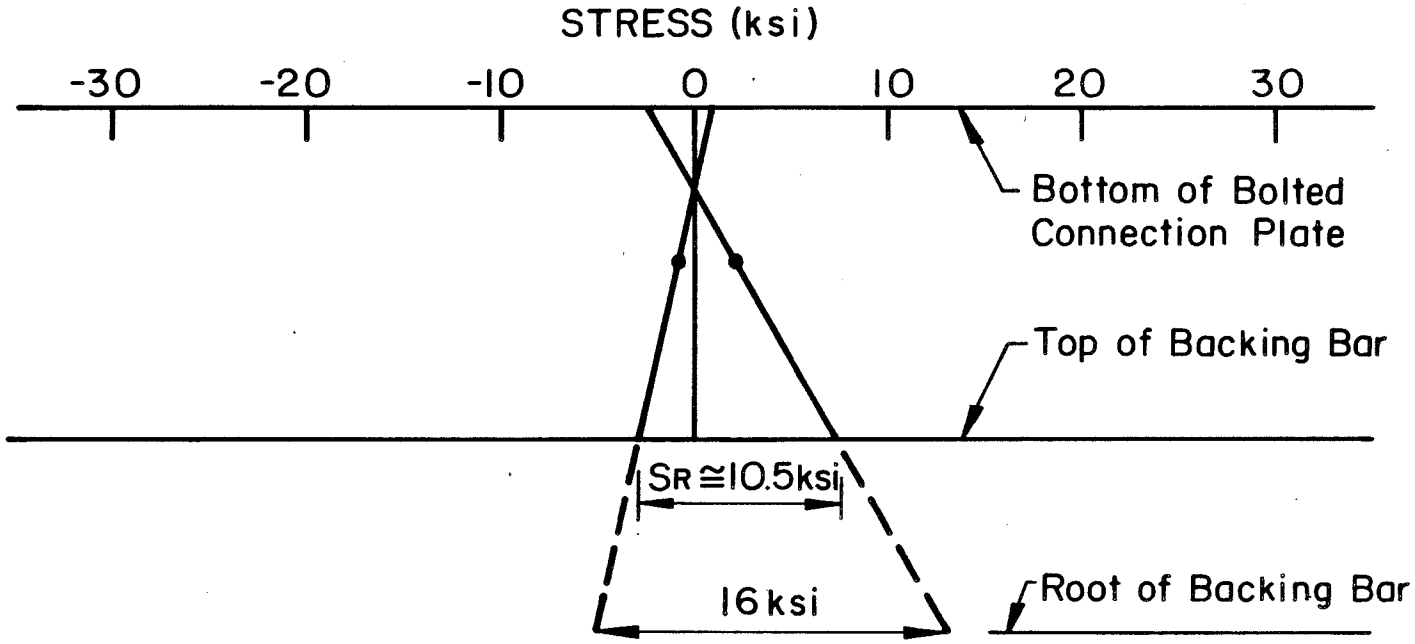

Fig. 29 Stress Gradient in Bottom Inside Web Gap at Panel Point 14

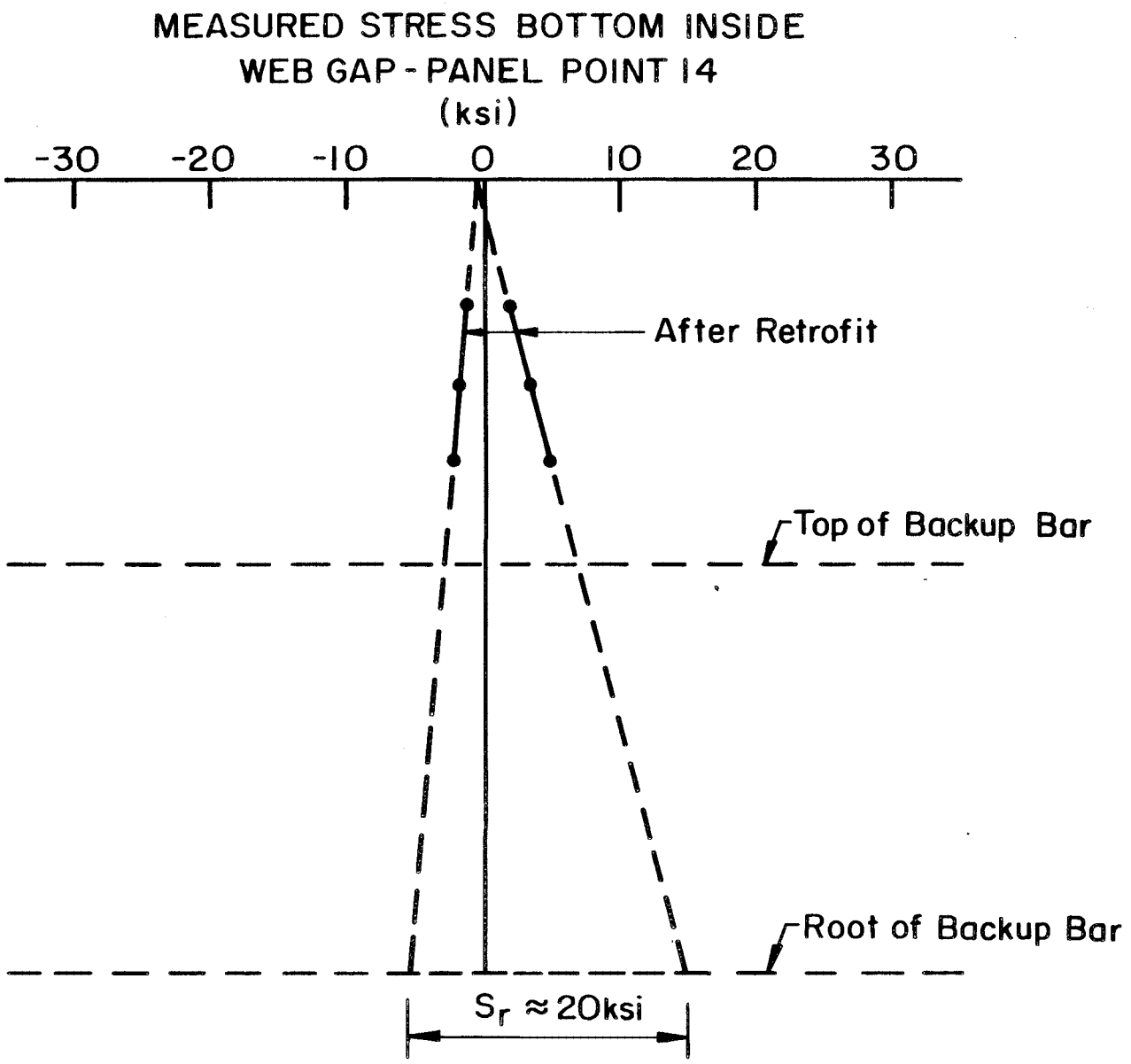

Fig. 30 Stress Gradient in the Bottom Inside Web Gap at Panel Point 14

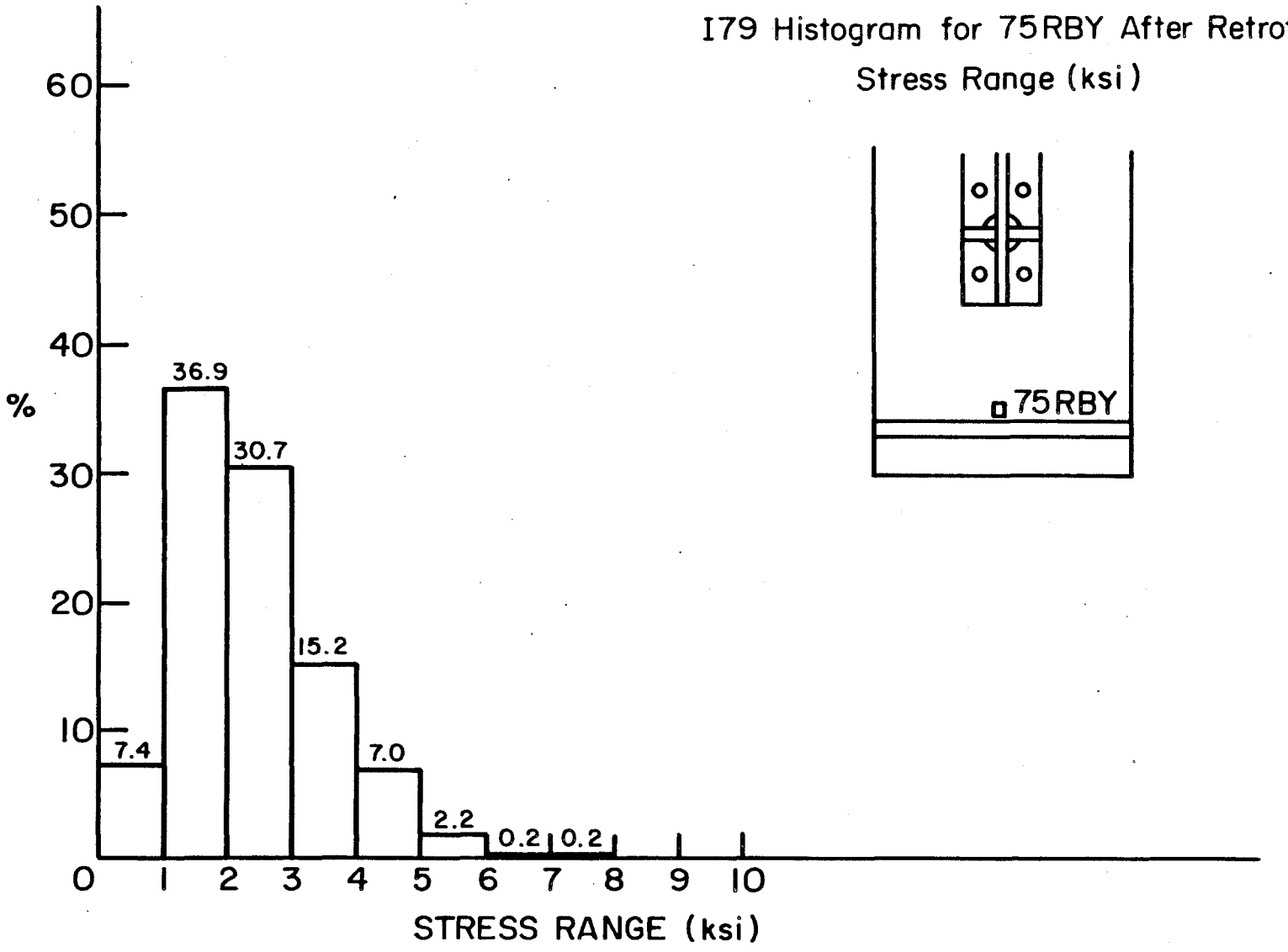

Fig. 31 Stress Range Histograph for Gage on Bottom Inside Web Gap

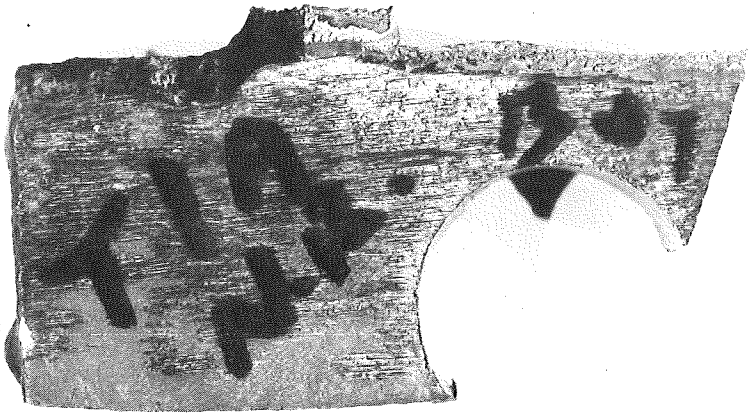

Fig. 32 View of Sample Removed from Panel Point T1A-NB Bottom

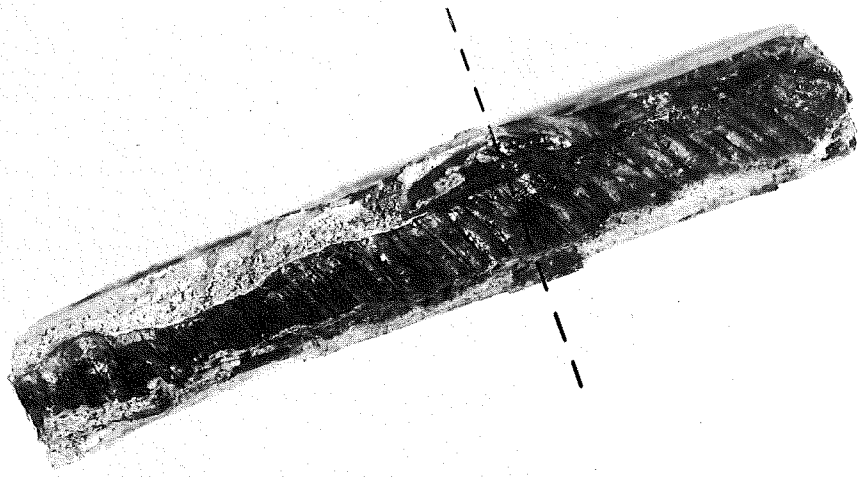

Fig. 33 View of Crack Surface of T1A-NB Bottom Showing Flame-Cut Edge of Diaphragm and Large Lack of Fusion

Fig. 34 View of Sample Removed from Panel Point T1A-NB Top

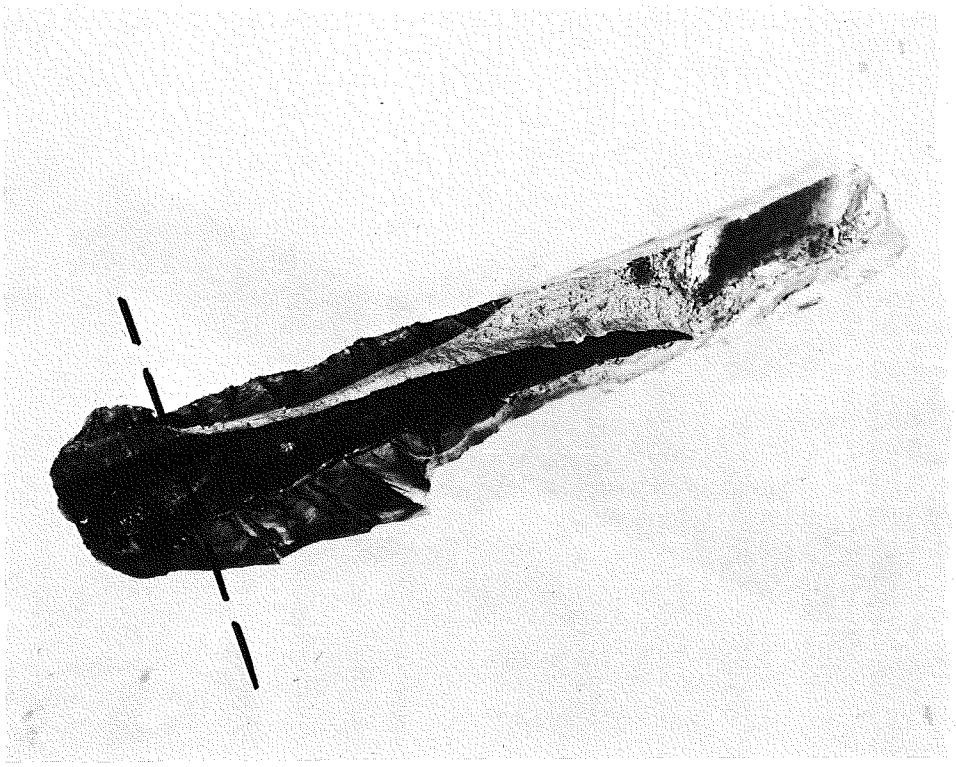

Fig. 35 Crack Surface of T1A-NB Top Showing Lack of Fusion and Fatigue Crack Growth

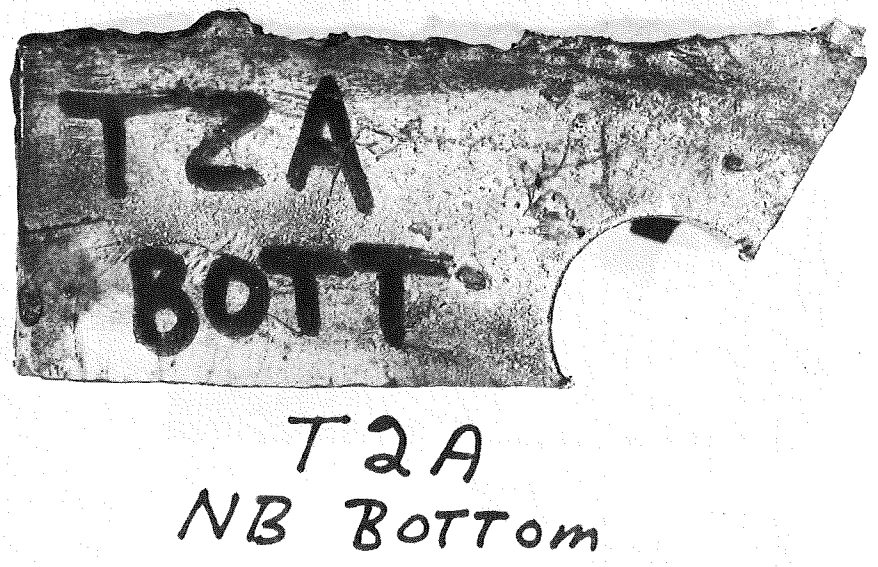

Fig. 36 View of Sample Removed from Panel Point T2A-NB Bottom

Fig. 37 Crack Surface of T2A-NB Bottom
Showing No Significant Fusion

Fig. 38 View of Sample Removed from Panel Point T2A-NB Top

Fig. 39 Crack Surface Showing Large Lack of Fusion Area and Fatigue Crack Where Fused

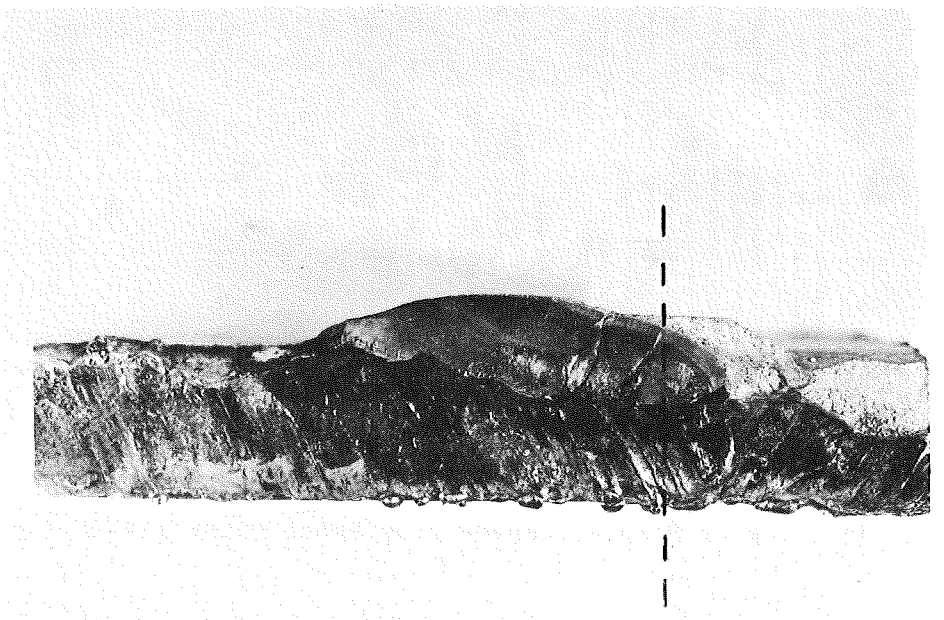

Fig. 40 Close-Up View of Fatigue Crack
at Small Fused Area

Fig. 41 View of Sample Removed from T4-NB Bottom

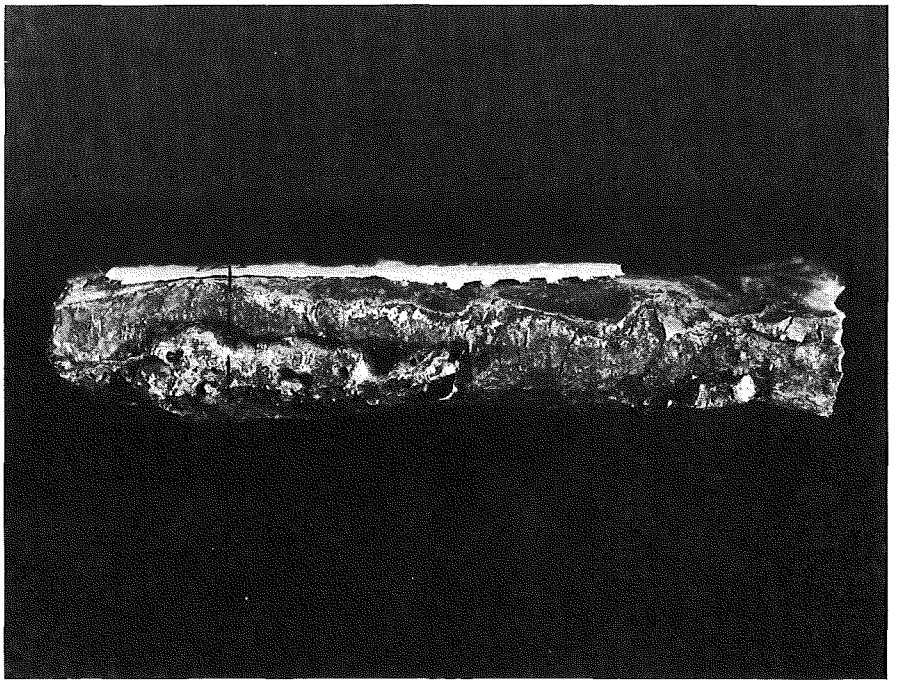

Fig. 42 View of Crack Surface Showing Lack of Fusion

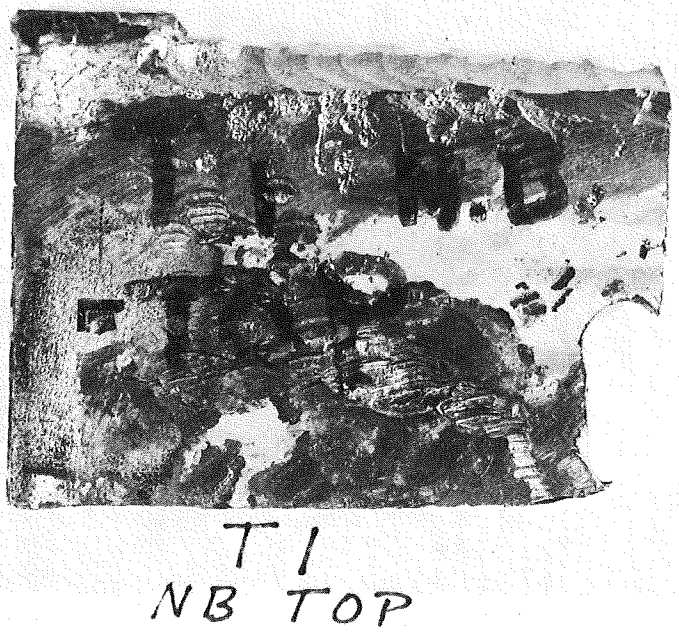

Fig. 43 View of Sample From Panel Point T1-NB Top

Fig. 44 Crack Surface of T1-NB Top

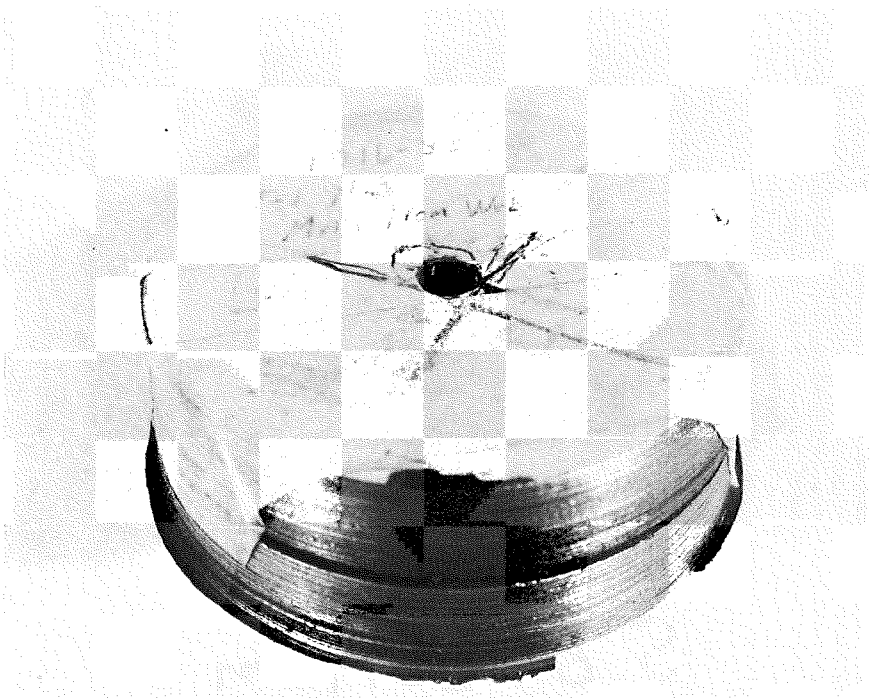

Fig. 45 Cores Removed from Hanger Splice Plate and Web at Panel Point T1-NB Top

Fig. 46 Inside Web Plate Surface at T1-NB Showing Cracks in Grooved Areas

Fig. 47 Sample Removed from Panel Point T4A-SB Bottom

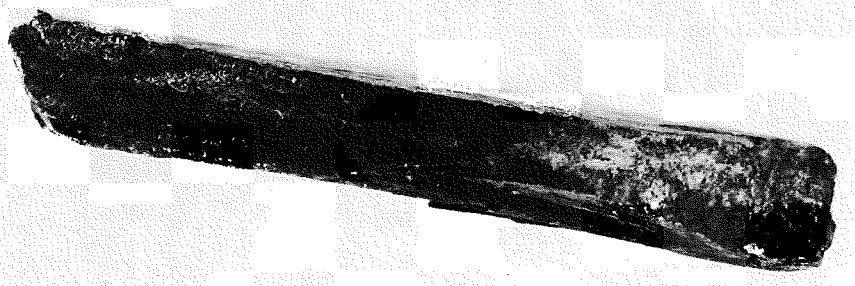

Fig. 48 Crack Surface at T4A-SB Bottom
Showing Large Unfused Areas

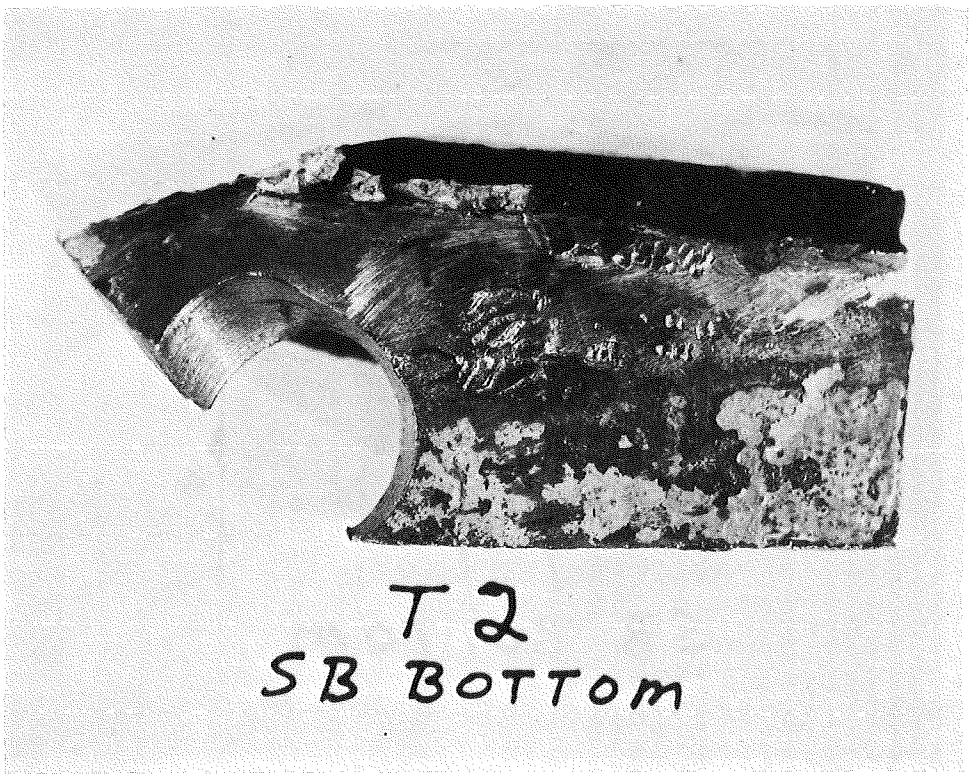

Fig. 49 Sample Removed at Panel Point T2-SB Bottom

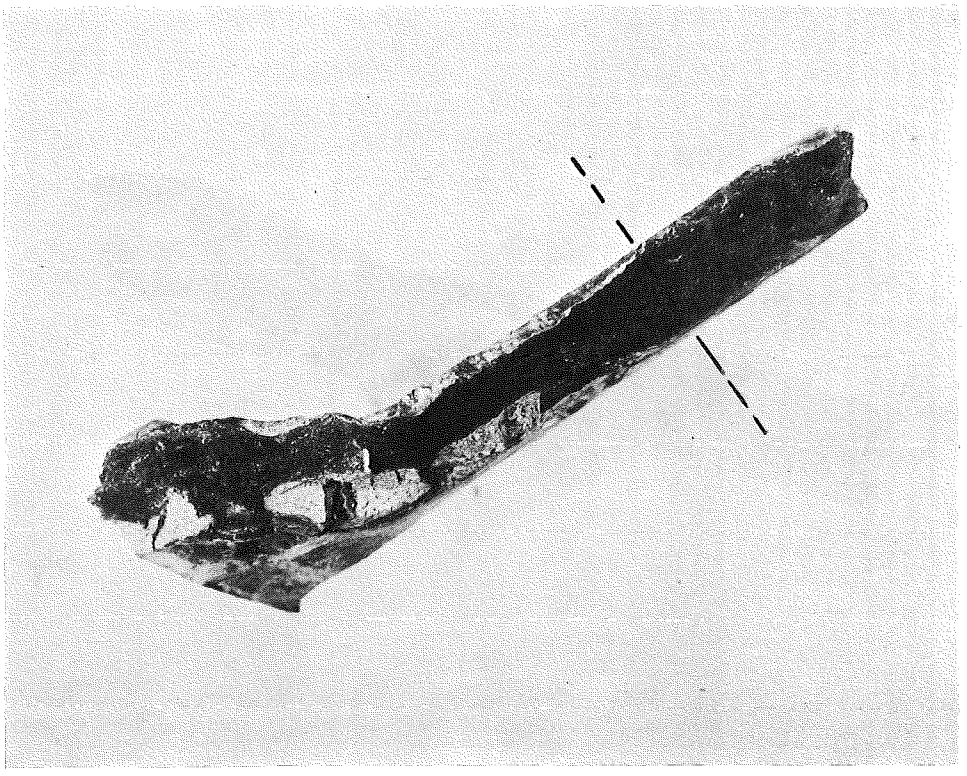

Fig. 50 Crack Surface Showing Large Lack of Fusion Region at End of Diaphragm

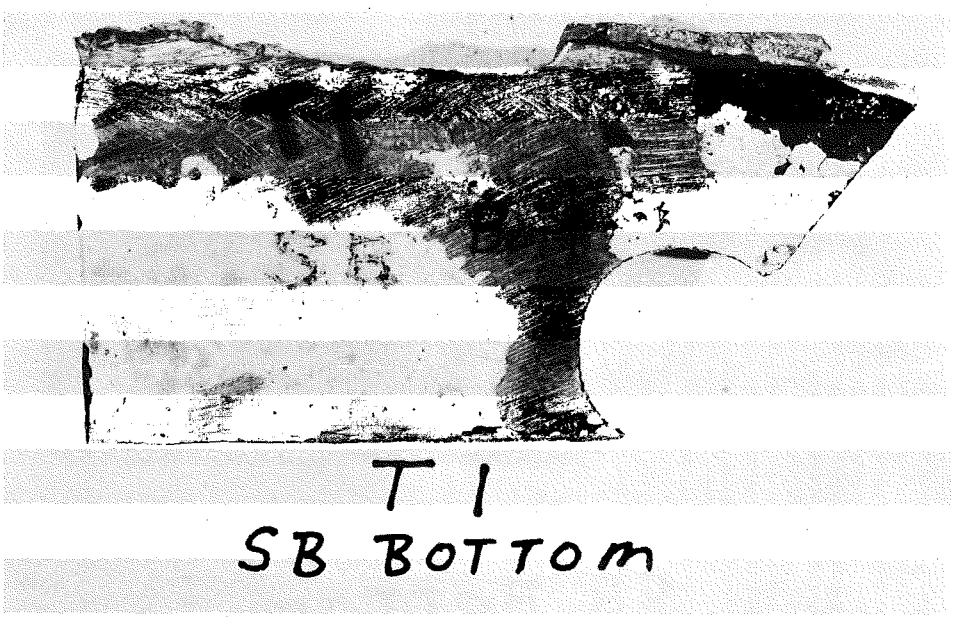

Fig. 51 Sample Removed from Panel Point T1-SB Bottom

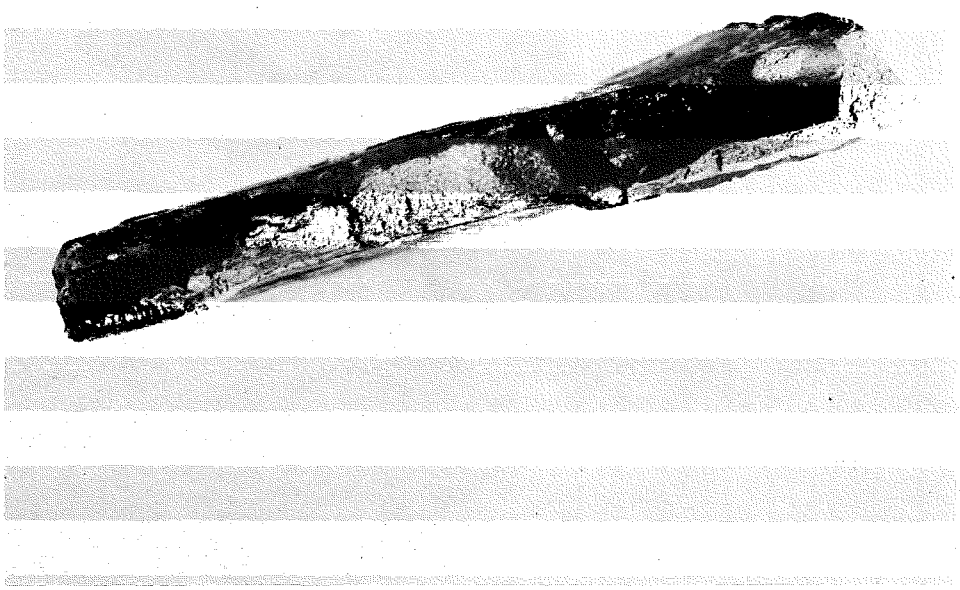

Fig. 52 Crack Surface Showing Large Lack of Fusion Regions

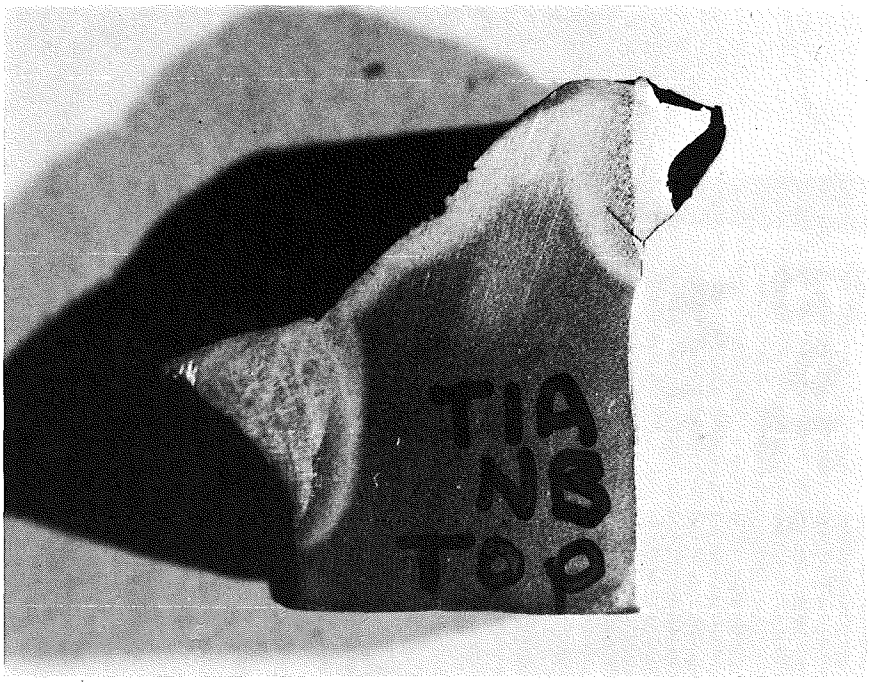

Fig. 53 Polished and Etched Section of T1A-NB Top Near End of Diaphragm (see Fig. 35)

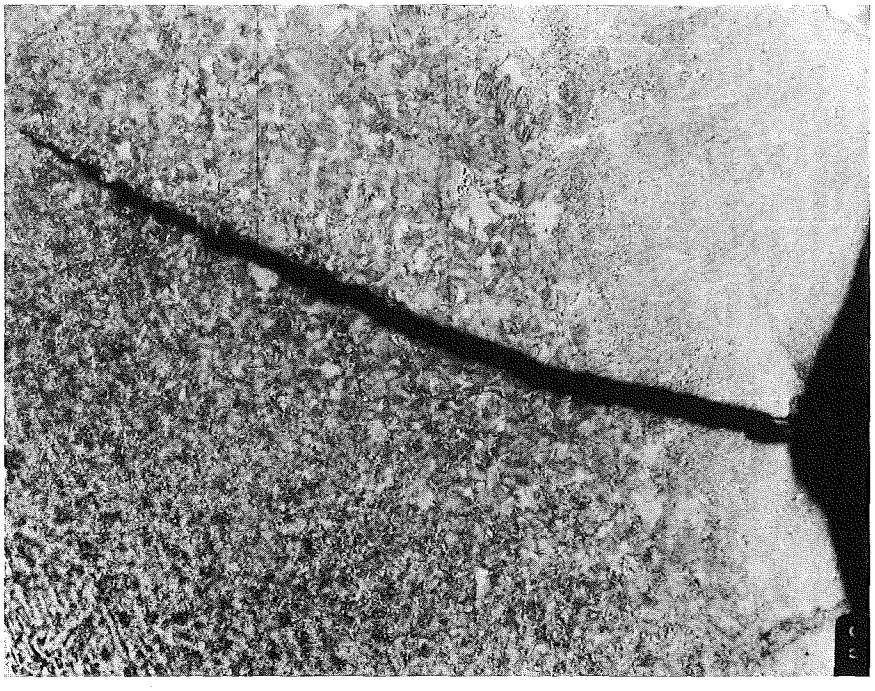

Fig. 54 Close-Up View of Secondary Crack Growing From Weld Toe (see Fig. 53) @ 40X

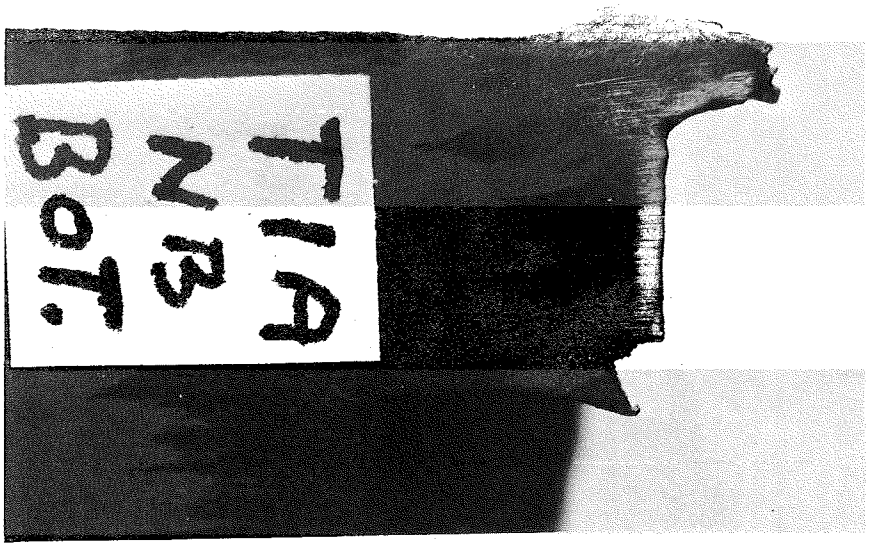

Fig. 55 Polished and Etched Section of T1A-NB Bottom Near End of Diaphragm (see Fig. 33)

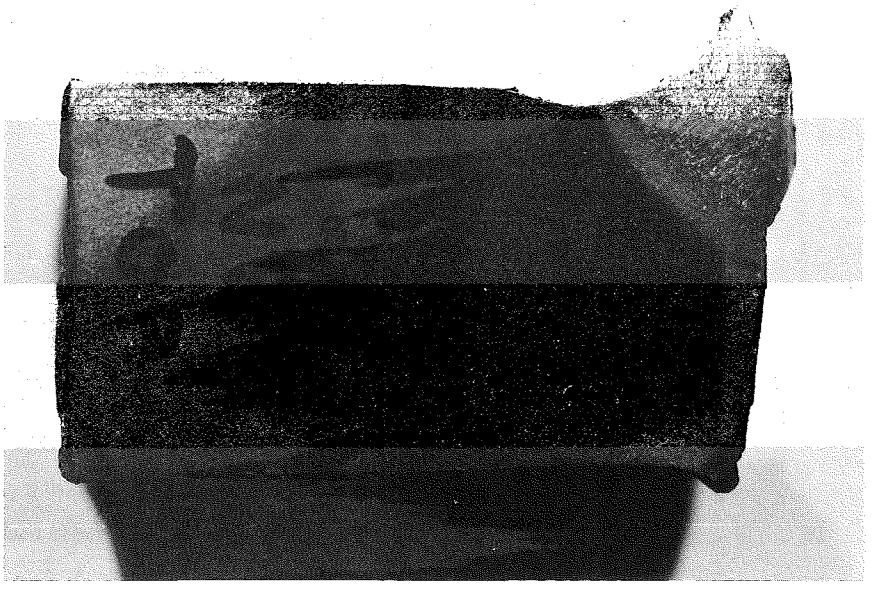

Fig. 56 Polished and Etched Section of T2A-NB Top (see Fig. 40)

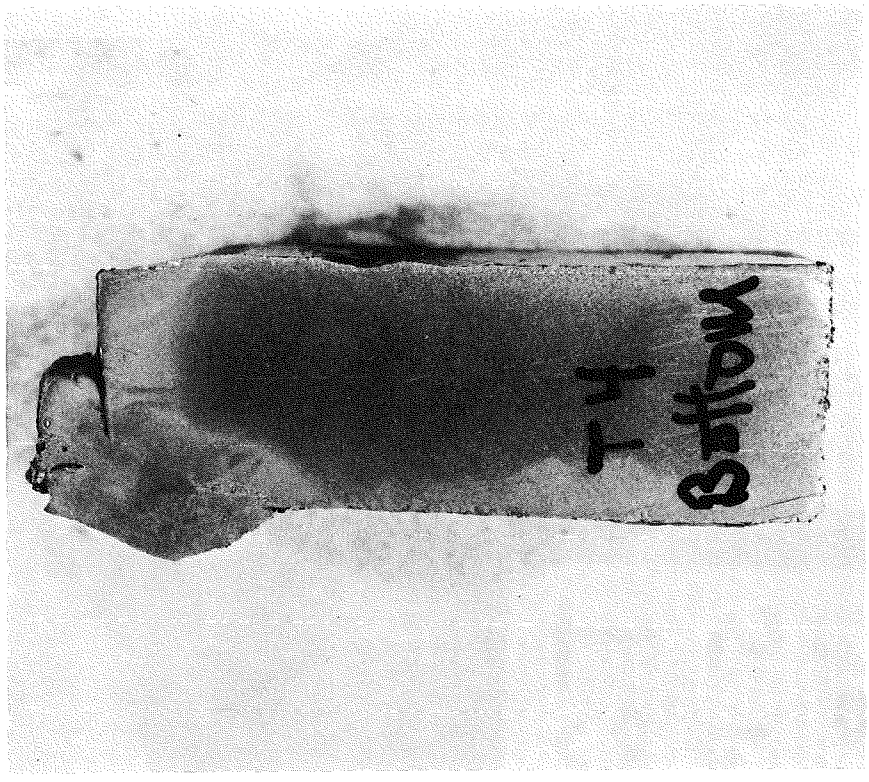

Fig. 57 Polished and Etched Section of T4-NB Bottom
(See Fig. 42)

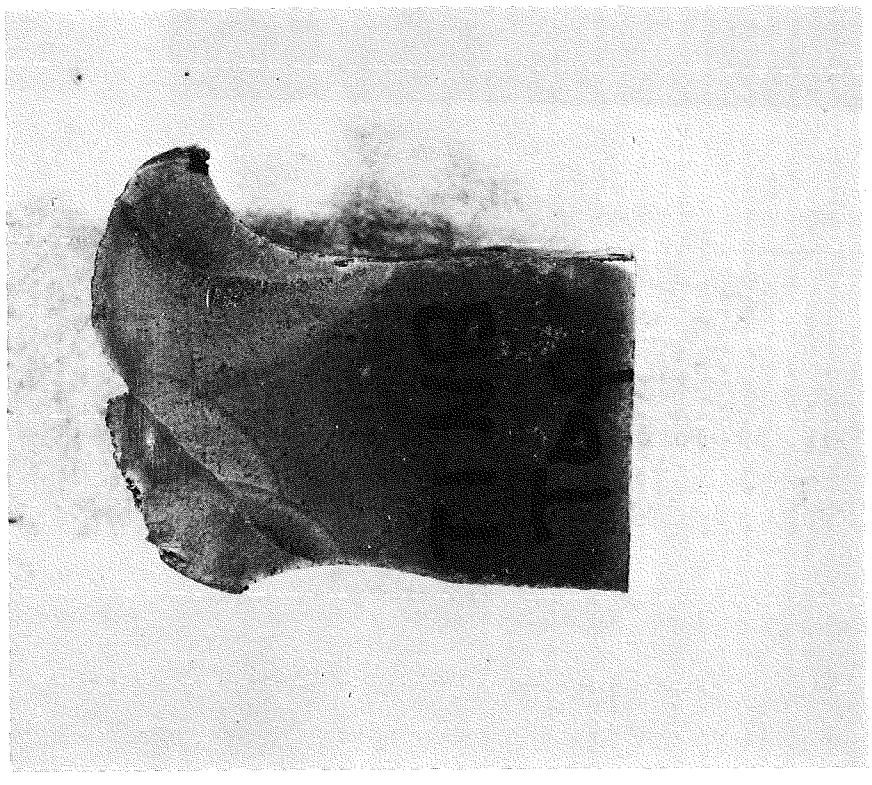

Fig. 58 Polished and Etched Section of T1-NB Top
(See Fig. 44)

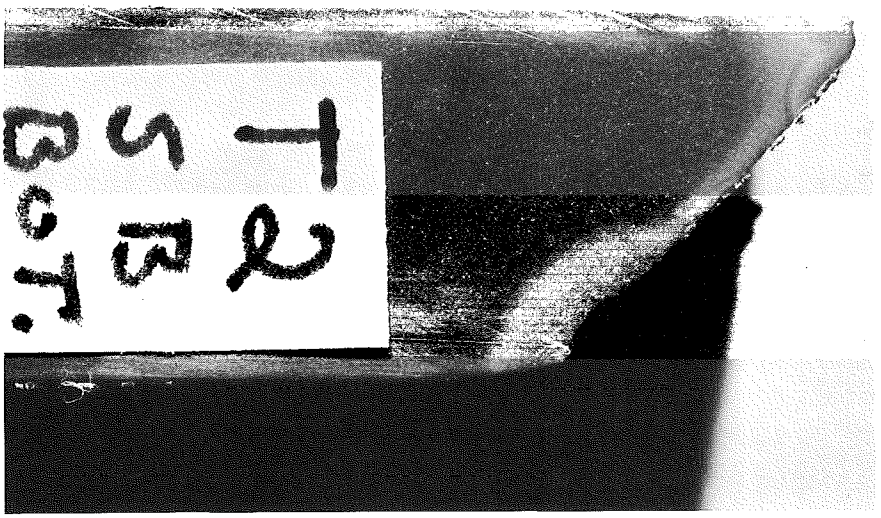

Fig. 59 Polished and Etched Section of T2-SB Bottom
(See Fig. 50)

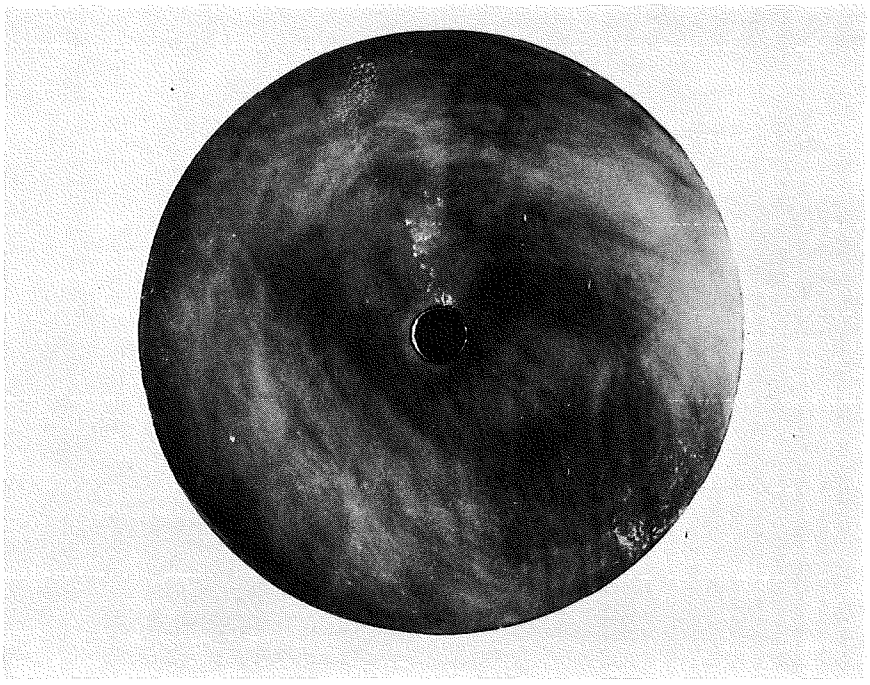

Fig. 60 Milled and Polished Surface of Core from T1-NB

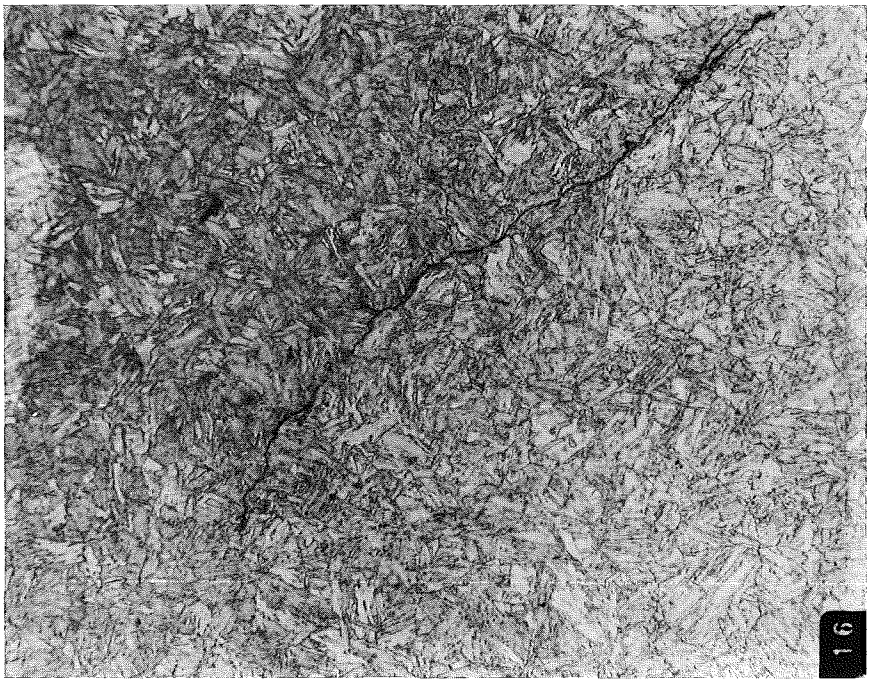

Fig. 61 Fatigue Crack Tip at Midthickness of Web Plate at 500X

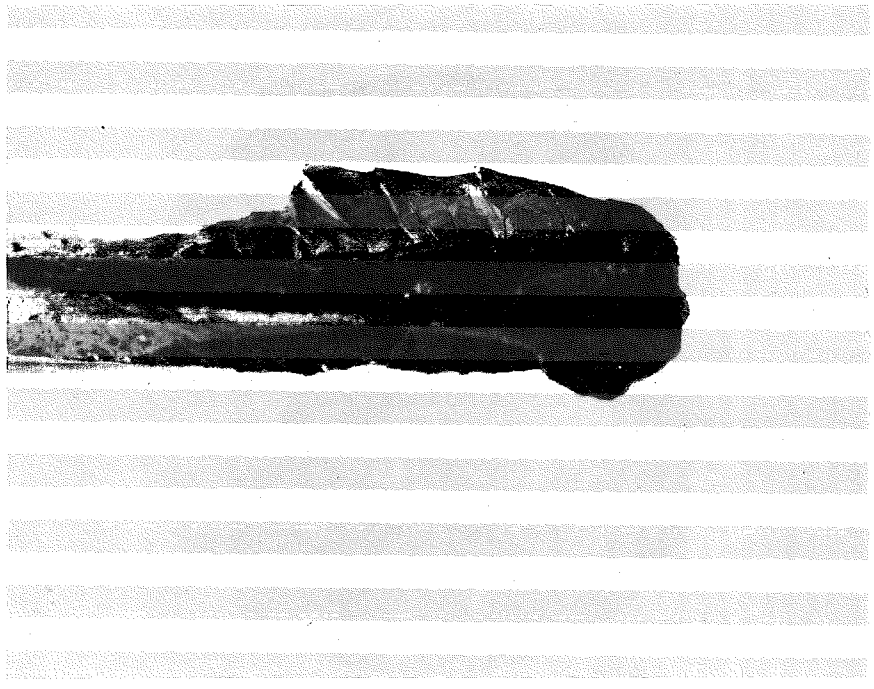

Fig. 62 Location of SEM Studies on T1A-NB Top

Fig. 63 SEM Fractograph @ 20X Showing Beachmarks on Crack Surface

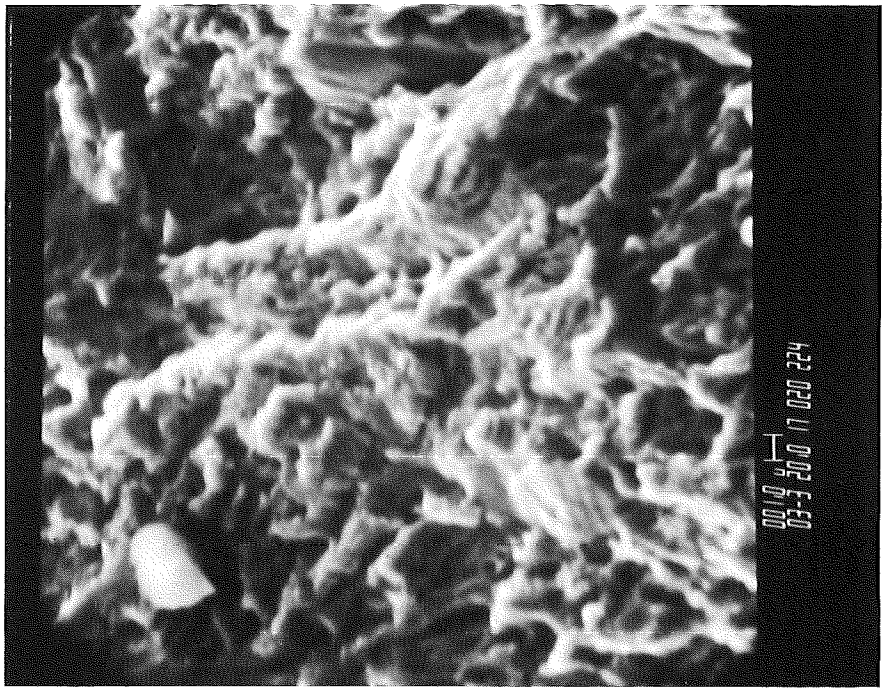

Fig. 64 SEM Fractograph @ 3000X Showing Corrosion Product and Striation-like Features at Black Dot Marked in Fig. 63

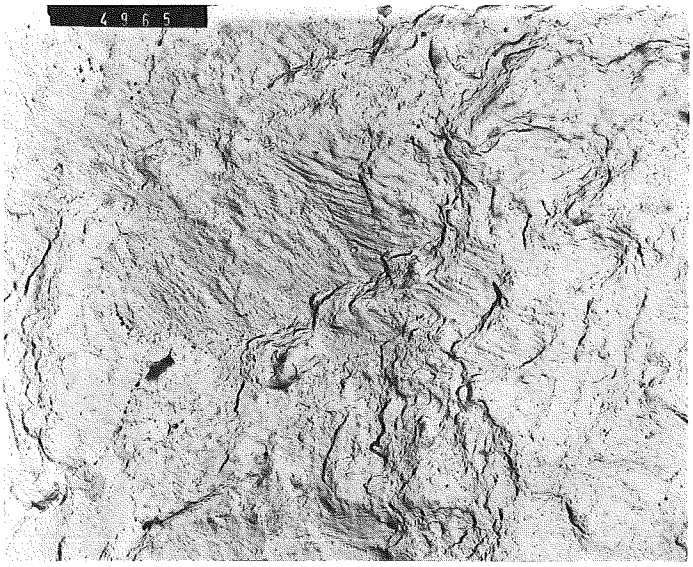

Fig. 65 TEM Fractograph at 6300X Showing Striation Features on Crack Surface of T1A-NB Top

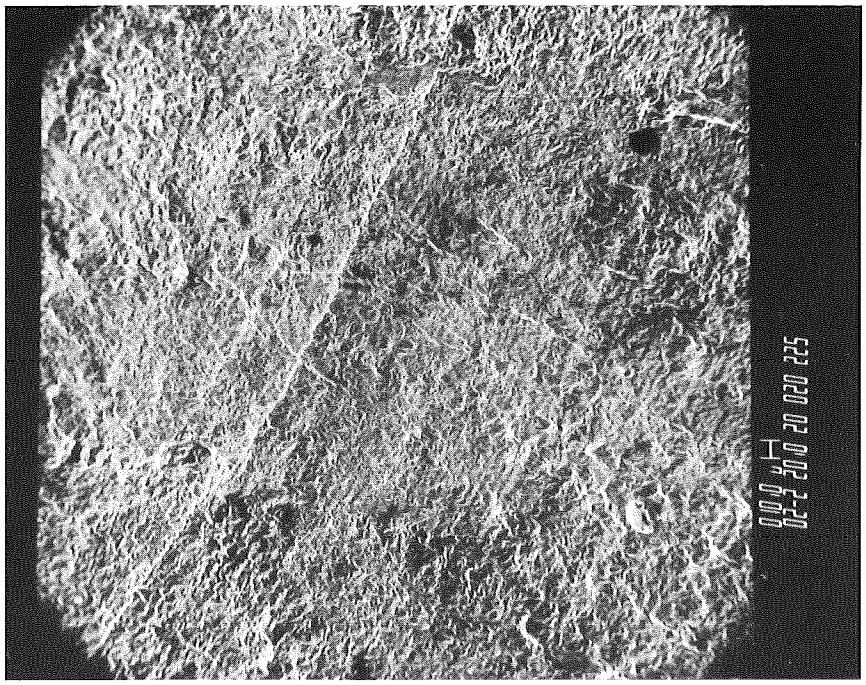

Fig. 66 SEM Fractograph of Fatigue Crack Surface Shown in Fig. 40 @ 20X Showing Beachmarks on T2A-NB Top

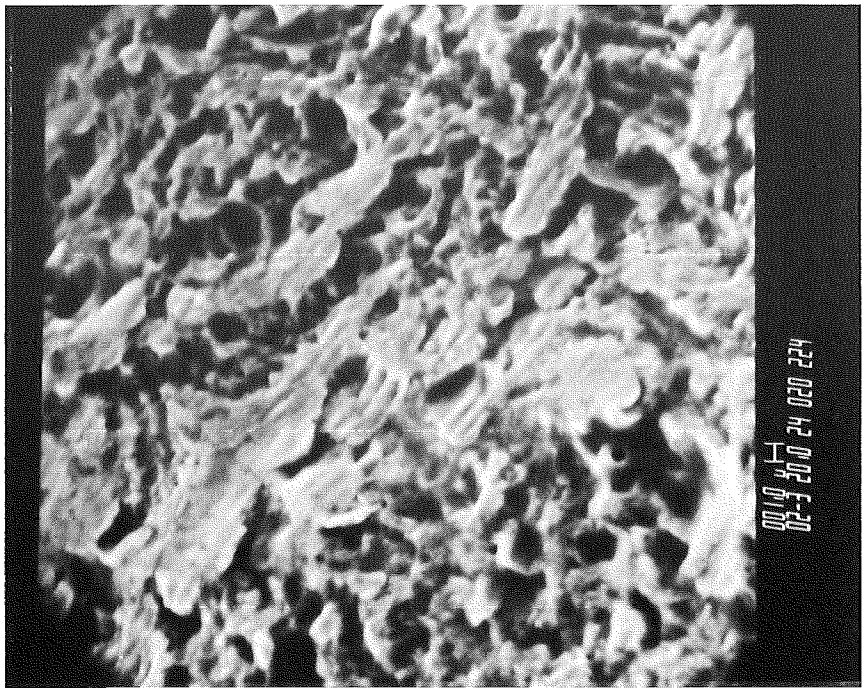

Fig. 67 SEM Fractograph at 2000X Showing Striation-like Features

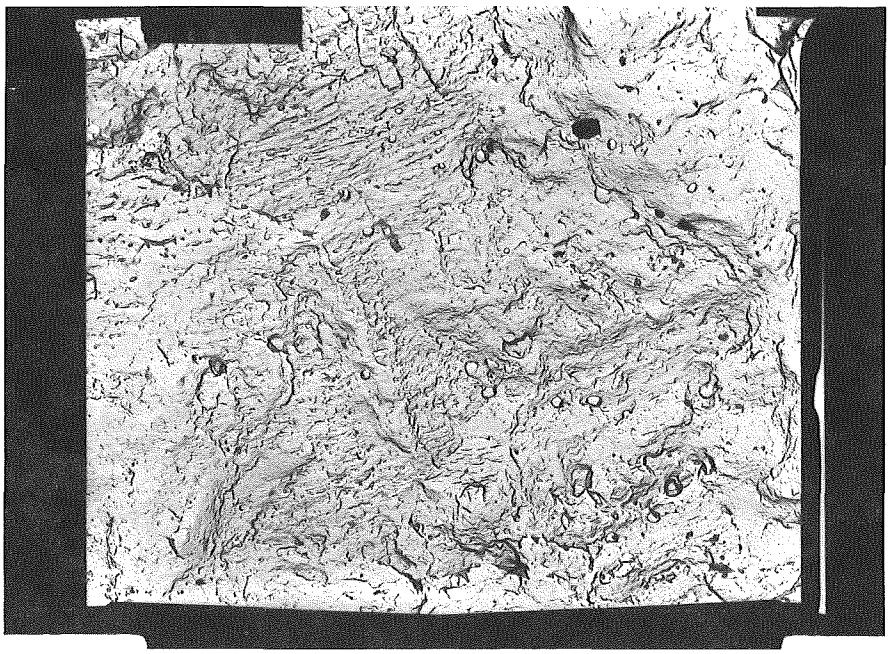

Fig. 68 TEM Fractograph at 7800X Showing Striation Features on Crack Surface of T2A-NB Top

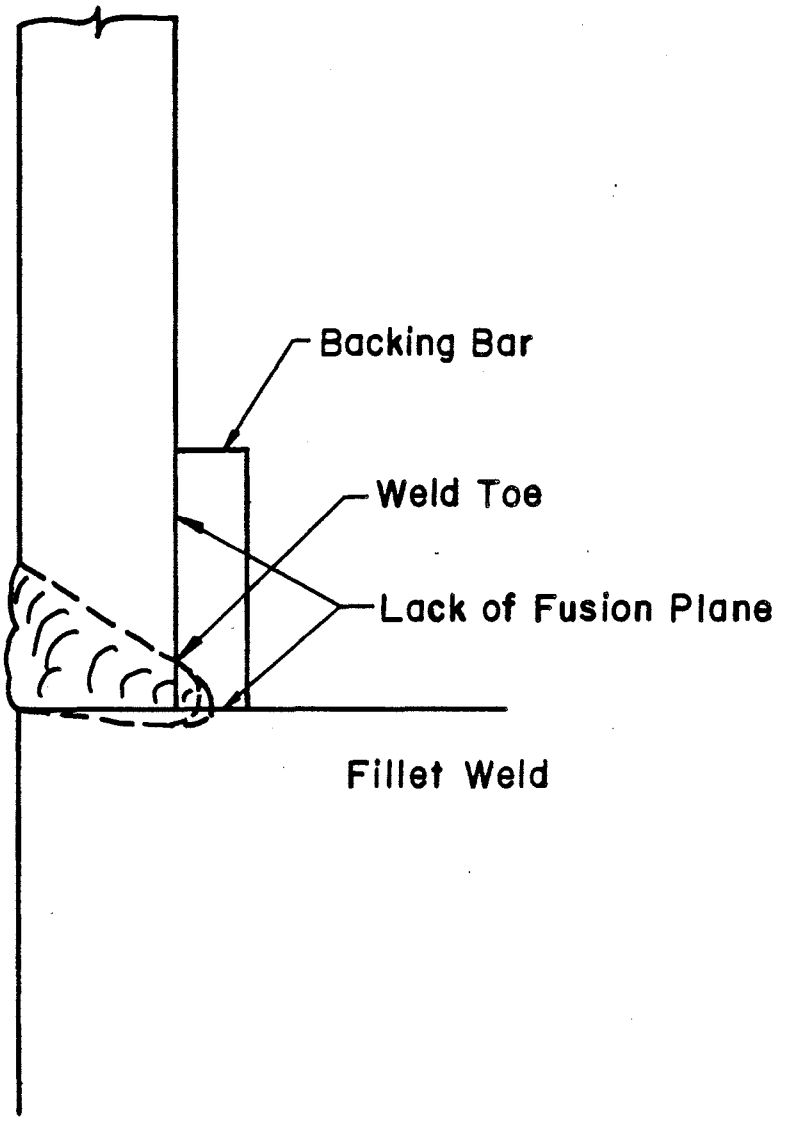

Fig. 69 Schematic of Box Corner Weld and Backing Bar Showing Lack of Fusion Planes

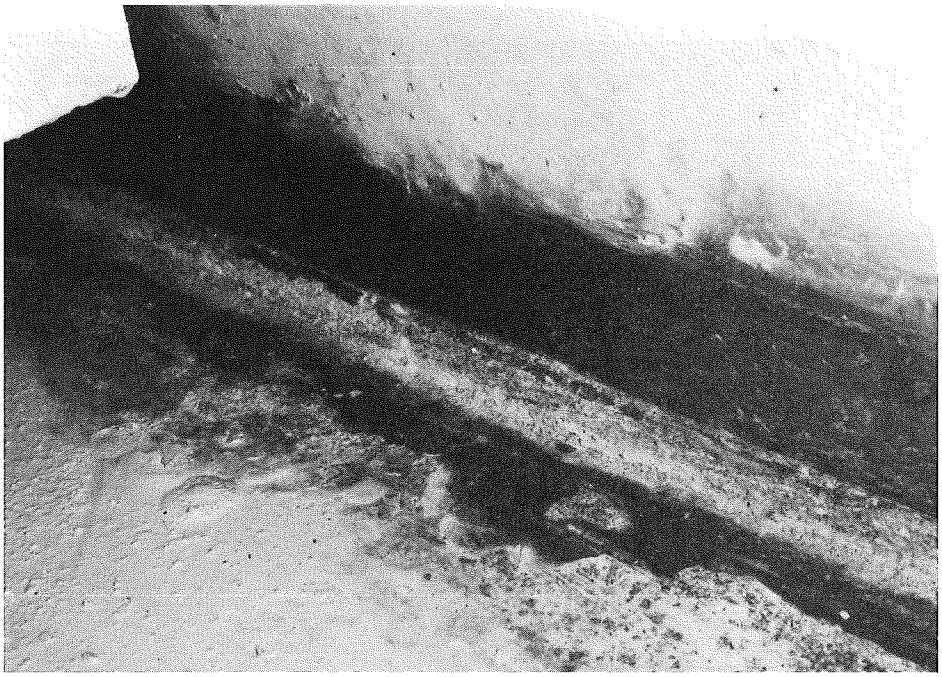

Fig. 70 Weld in Box Corner after Removal of Backing Bar

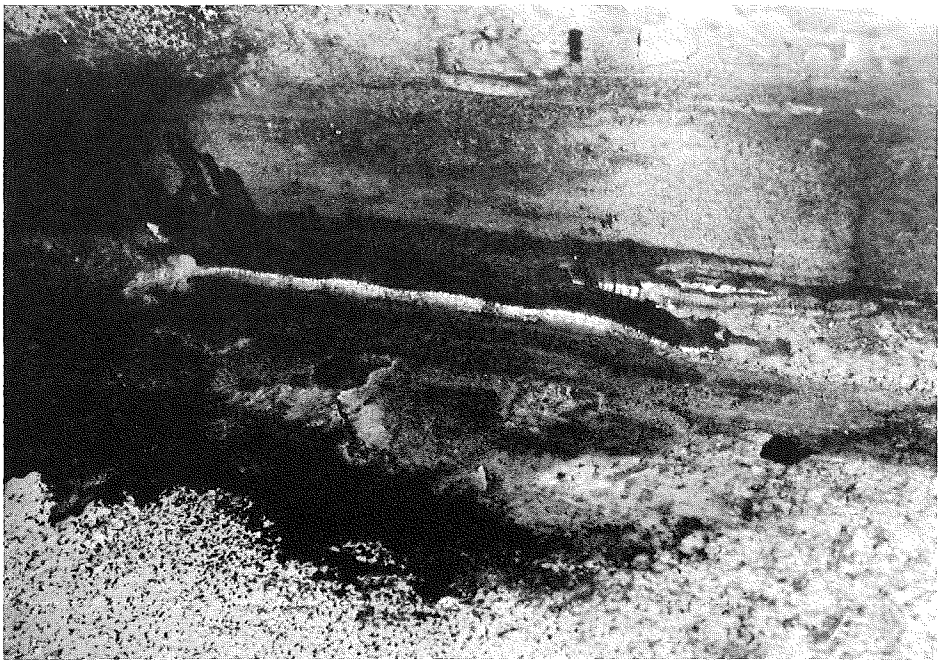

Fig. 71 Weld Toe Regions on Web and at Flange After Grinding

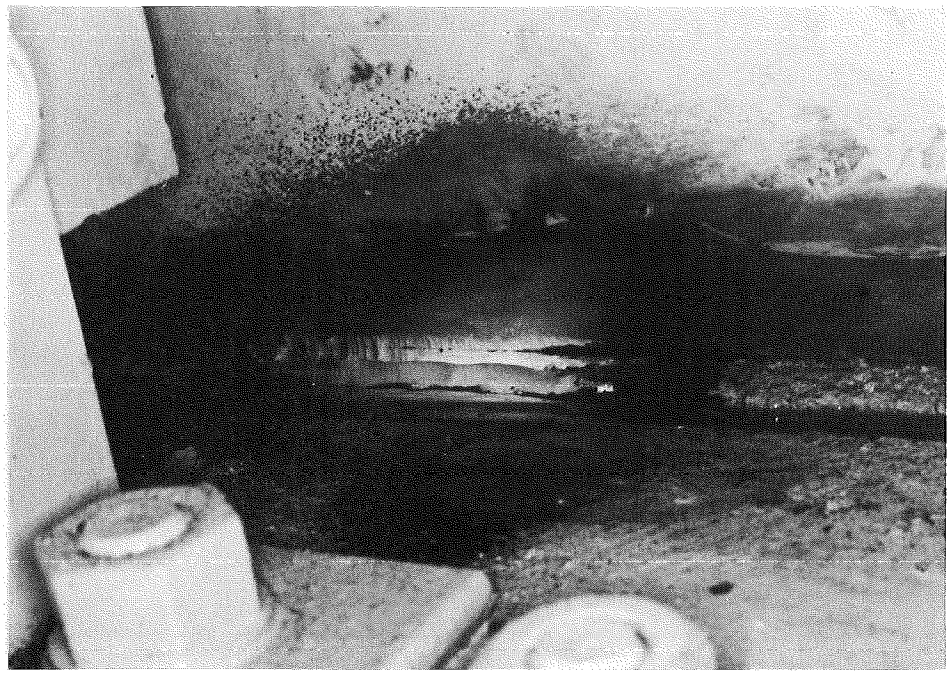

Fig. 72 Region in Gap After Application of Liquid Penetrant

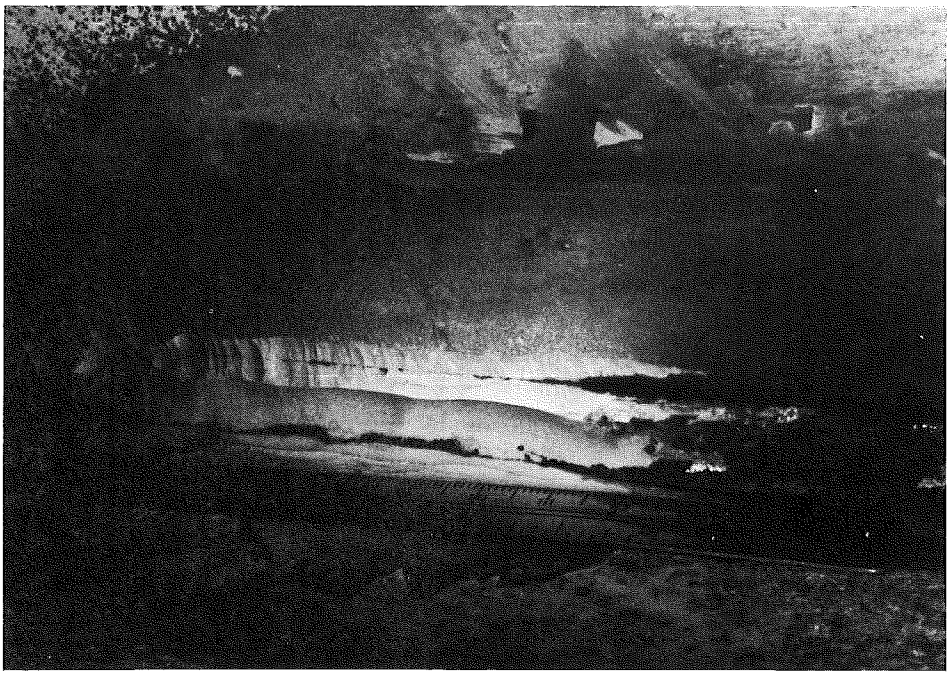

Fig. 73 Cracks Can Be Seen in Web Plate at "Weld Toe" and From Plane at Flange Surface

Fig. 74 Crack-like Indication in the Web Plate at Termination of Backing Bar

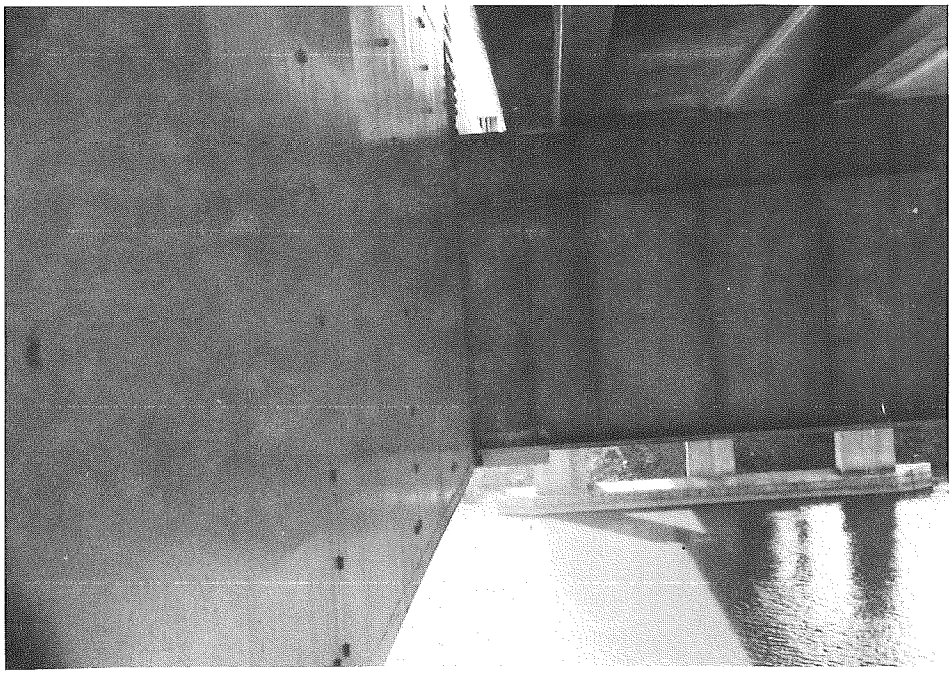

Fig. 75 Splice Plate Installed Between Bottom Flange of Floor Beam and Tie Girder